Reconciling leaf physiological traits and canopy flux data: Use of the TRY and FLUXNET databases in the Community Land Model version 4

Gordon B. Bonan,[1] Keith W. Oleson,[1] Rosie A. Fisher,[1] Gitta Lasslop,[2,3] and Markus Reichstein[2]

Received 23 November 2011; revised 17 April 2012; accepted 5 May 2012; published 20 June 2012.

[1] The Community Land Model version 4 overestimates gross primary production (GPP) compared with estimates from FLUXNET eddy covariance towers. The revised model of Bonan et al. (2011) is consistent with FLUXNET, but values for the leaf-level photosynthetic parameter $V_{c\max}$ that yield realistic GPP at the canopy-scale are lower than observed in the global synthesis of Kattge et al. (2009), except for tropical broadleaf evergreen trees. We investigate this discrepancy between $V_{c\max}$ and canopy fluxes. A multilayer model with explicit calculation of light absorption and photosynthesis for sunlit and shaded leaves at depths in the canopy gives insight to the scale mismatch between leaf and canopy. We evaluate the model with light-response curves at individual FLUXNET towers and with empirically upscaled annual GPP. Biases in the multilayer canopy with observed $V_{c\max}$ are similar, or improved, compared with the standard two-leaf canopy and its low $V_{c\max}$, though the Amazon is an exception. The difference relates to light absorption by shaded leaves in the two-leaf canopy, and resulting higher photosynthesis when the canopy scaling parameter K_n is low, but observationally constrained. Larger K_n decreases shaded leaf photosynthesis and reduces the difference between the two-leaf and multilayer canopies. The low model $V_{c\max}$ is diagnosed from nitrogen reduction of GPP in simulations with carbon-nitrogen biogeochemistry. Our results show that the imposed nitrogen reduction compensates for deficiency in the two-leaf canopy that produces high GPP. Leaf trait databases ($V_{c\max}$), within-canopy profiles of photosynthetic capacity (K_n), tower fluxes, and empirically upscaled fields provide important complementary information for model evaluation.

Citation: Bonan, G. B., K. W. Oleson, R. A. Fisher, G. Lasslop, and M. Reichstein (2012), Reconciling leaf physiological traits and canopy flux data: Use of the TRY and FLUXNET databases in the Community Land Model version 4, *J. Geophys. Res.*, *117*, G02026, doi:10.1029/2011JG001913.

1. Introduction

[2] Models of the terrestrial biosphere for climate simulation have evolved from an initial hydrometeorological framework for energy and water fluxes to include biogeochemical cycles of carbon and nitrogen [*Bonan*, 2008]. The geophysical and ecological data sets with which to evaluate these models have evolved in tandem with model capability. Eddy covariance measurements of sensible heat flux, latent heat flux, and CO_2 flux are routinely used to evaluate models and to inform model development at individual or multiple tower sites [*Randerson et al.*, 2009; *Lawrence et al.*, 2011; *Blyth et al.*, 2011; *Wang et al.*, 2011]. With the advent of global flux data sets derived from individual tower sites [*Jung et al.*, 2010, 2011; *Beer et al.*, 2010], the models can now be confronted with data of biosphere functioning at the global scale [*Bonan et al.*, 2011].

[3] Estimation of required model parameters is not straightforward, especially for global simulations. For example, global terrestrial biosphere models commonly use a variant of the *Farquhar et al.* [1980] photosynthesis model coupled to the Ball-Berry stomatal conductance model [*Ball et al.*, 1987; *Collatz et al.*, 1991]. A key term in these equations is the photosynthetic parameter $V_{c\max}$. This leaf-level parameter describes the maximum rate of carboxylation by the photosynthetic enzyme Rubisco. Various synthesis data sets for $V_{c\max}$ have been developed for use in global models [*Wullschleger*, 1993; *Beerling and Quick*, 1995]. Most recently, *Kattge et al.* [2009] derived values for $V_{c\max}$ at standardized temperature (25°C) based on a meta-analysis of

[1]National Center for Atmospheric Research, Boulder, Colorado, USA.
[2]Max Planck Institute for Biogeochemistry, Jena, Germany.
[3]Now at Max Planck Institute for Meteorology, Hamburg, Germany.

Corresponding author: G. Bonan, National Center for Atmospheric Research, PO Box 3000, Boulder, CO 80307, USA. (bonan@ucar.edu)

©2012. American Geophysical Union. All Rights Reserved.
0148-0227/12/2011JG001913

photosynthetic measurements extrapolated to field vegetation using observed foliage nitrogen content, and those values are included in the TRY global database of plant traits [*Kattge et al.*, 2011]. However, values for V_{cmax} can differ greatly among terrestrial biosphere models, in part because model structural errors are compensated by parameter adjustment [*Bonan et al.*, 2011].

[4] Simulations with the Community Land Model (CLM) highlight the discrepancy between leaf traits and canopy fluxes. *Bonan et al.* [2011] showed that CLM version 4 (CLM4) overestimates gross primary production (GPP) compared with estimates from the FLUXNET network of eddy covariance tower sites. A revised model with improved radiative transfer for sunlit and shaded leaves, leaf photosynthesis and stomatal conductance, and canopy scaling of leaf photosynthesis is consistent with FLUXNET-derived GPP (and also evapotranspiration). The values used for V_{cmax} in both CLM4 and the revised model, however, are mostly much lower than the *Kattge et al.* [2009] synthesis.

[5] Here, we extend the model development of *Bonan et al.* [2011] and further revise CLM4 to improve its simulation of GPP. In doing so, we illustrate how data sets of leaf physiological traits and canopy fluxes can be used together to test and improve global terrestrial biosphere models. One methodology for parameter estimation, particularly with respect to V_{cmax}, is to derive effective parameter values from canopy-scale eddy covariance flux measurements [*Wang et al.*, 2001, 2007; *Santaren et al.*, 2007; *Williams et al.*, 2009; *Ziehn et al.*, 2011]. This approach explicitly recognizes the difficulty in applying parameter values obtained at the leaf-level to larger scales. In contrast, we constrain V_{cmax} from global leaf trait syntheses [*Kattge et al.*, 2009] to explicitly test our understanding of leaf to canopy scaling of photosynthetic processes. We use a multilayer canopy model and compare this to a two-leaf sunlit/shaded canopy parameterization to investigate the discrepancy between leaf traits and flux data.

[6] Our results have important implications for the parameterization of carbon-nitrogen biogeochemistry in CLM4 (denoted CLM4CN) [*Thornton et al.* 2007, 2009], because the low V_{cmax} values used in CLM4 are diagnosed from the simulated reduction of GPP by nitrogen in CLM4CN. We show that the simulated nitrogen reduction compensates for deficiencies in the two-leaf canopy parameterization that make the model too productive.

2. Methods

2.1. Model Description

[7] The CLM4 is a canopy-integrated model that represents the plant canopy as two big leaves – a sunlit leaf and a shaded leaf [*Oleson et al.*, 2010; *Lawrence et al.*, 2011]. The model has large positive biases in GPP and evapotranspiration compared with FLUXNET data, and we use the revised model described by *Bonan et al.* [2011]. This model is a variant of CLM4, but with: a revised two-stream radiative transfer parameterization to account for sunlit and shaded fractions of the canopy [*Dai et al.*, 2004]; an updated version of the *Farquhar et al.* [1980] photosynthesis model for C_3 plants, the *Collatz et al.* [1992] C_4 photosynthesis model, and the Ball-Berry stomatal conductance model [*Ball et al.*, 1987; *Collatz et al.*, 1991]; and canopy scaling of leaf photosynthetic properties based on an exponential profile of foliage nitrogen with depth in the canopy [*Leuning et al.*, 1995]. These revisions greatly improve simulated GPP and evapotranspiration compared with global flux fields empirically inferred from FLUXNET data.

[8] In CLM4, V_{cmax} at 25°C is specified for each plant functional type from prescribed, time-invariant foliage nitrogen concentration [*Thornton and Zimmermann*, 2007] and is used to calculate potential GPP in the absence of nitrogen limitation. With prognostic carbon-nitrogen biogeochemistry (the CLM4CN model version), the model additionally diagnoses the availability of mineral nitrogen to support new plant growth, and the potential GPP is decreased if there is insufficient nitrogen to maintain required plant C:N stoichiometry (described in Text S1 of *Thornton et al.* [2007]). This nitrogen-induced reduction of GPP is applied after the photosynthesis calculation and is independent of V_{cmax}, but does implicitly decrease V_{cmax}. An effective V_{cmax} can be derived to match the nitrogen-decreased photosynthesis.

[9] Without carbon-nitrogen biogeochemistry, as in our simulations described here and in *Bonan et al.* [2011], the decrease in V_{cmax} is explicit. The potential V_{cmax} calculated from specified foliage nitrogen content is directly reduced by a prescribed nitrogen factor so that GPP is similarly decreased for nitrogen availability and is consistent with the GPP simulated by CLM4CN. This factor is scaled between zero and one to represent nitrogen constraints on photosynthesis, is time-invariant but does vary among plant functional types, and is derived from a CLM4CN simulation [*Bonan and Levis*, 2010; *Bonan et al.*, 2011].

[10] The reduction of potential GPP by nitrogen is a key feature of the model. Without it, simulated GPP is high, seen in CLM4 simulations without carbon-nitrogen biogeochemistry [*Bonan et al.*, 2011] and in CLM4CN simulations with prognostic carbon-nitrogen biogeochemistry [*Thornton et al.*, 2007, 2009; *Bonan and Levis*, 2010]. The decreased V_{cmax} values are much lower than the potential values without nitrogen reduction (Figure 1), and the quandary, as discussed by *Bonan et al.* [2011], is that the potential values for V_{cmax} before down-regulation are generally similar (or lower) to those reported by *Kattge et al.* [2009], which, as observed values under natural conditions, already reflect nitrogen limitation on photosynthetic rates. Here, we use the model in its simplest configuration, without prognostic leaf area and carbon-nitrogen biogeochemistry, to investigate why the model requires low V_{cmax} and why it performs poorly with the *Kattge et al.* [2009] values.

2.2. Photosynthesis Model and V_{cmax}

[11] The photosynthetic parameter V_{cmax} is not a directly observable quantity, but rather is estimated by fitting the *Farquhar et al.* [1980] photosynthesis model to leaf gas exchange measurements. The obtained V_{cmax} depends on the form of the model used and the parameter values that describe Rubisco kinetics in the model. The revised photosynthesis model introduced by *Bonan et al.* [2011] is the same as that used by *Kattge et al.* [2009] to derive V_{cmax} from leaf gas exchange measurements, which itself follows from *Medlyn et al.* [2002]. This form of the model does not distinguish the intercellular CO_2 concentration (c_i) and the chloroplastic CO_2 concentration (c_c), essentially assuming infinite conductance between the intercellular space and the site of carboxylation. This mesophyll conductance may, in

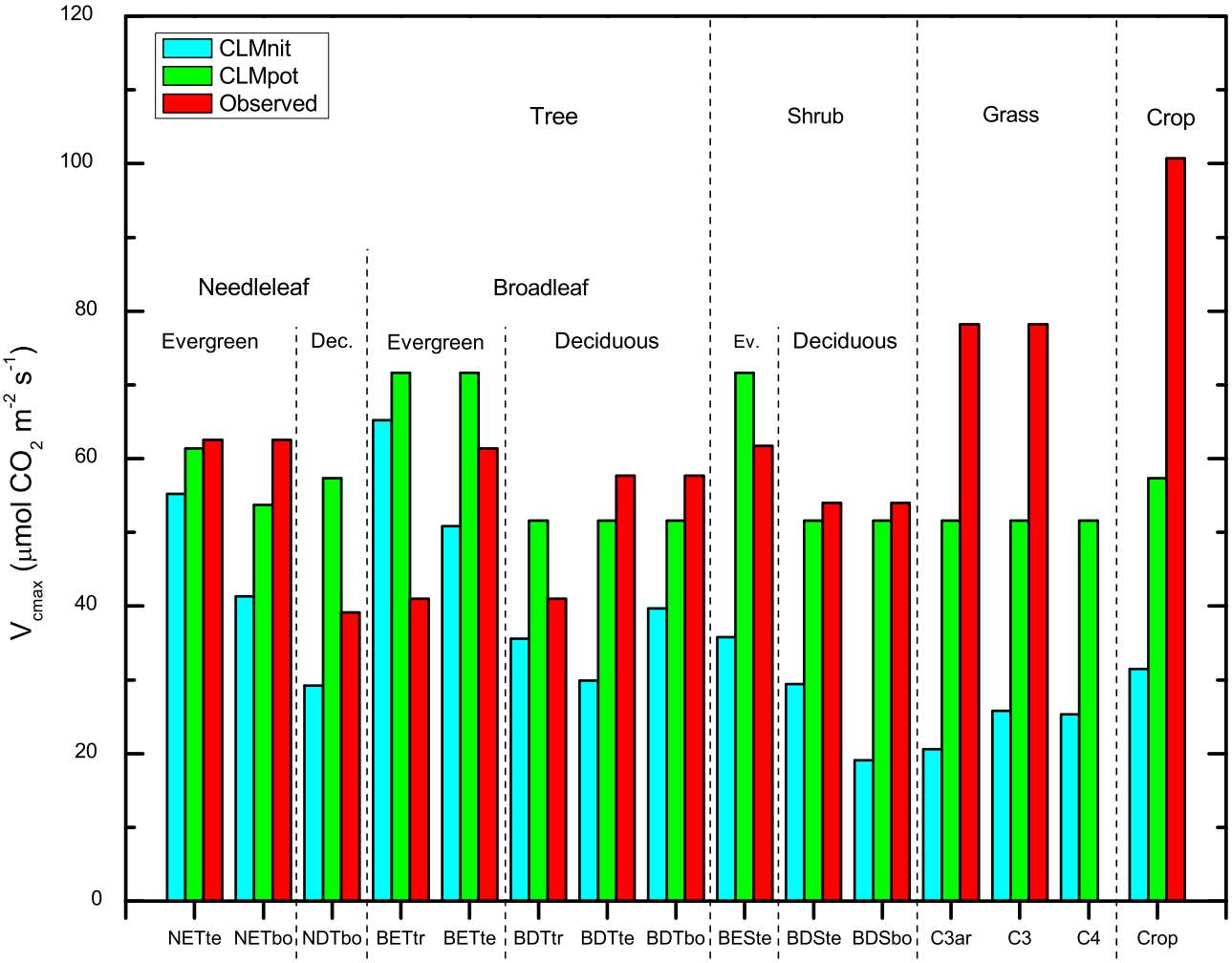

Figure 1. Values for V_{cmax} at 25°C used in model simulations compared with observed values for field vegetation [*Kattge et al.*, 2009]. Model values are shown without nitrogen reduction (CLMpot) and with inferred nitrogen reduction (CLMnit). These values are the $V^{opt}_{cmax\ 25}$ in *Bonan et al.* [2011, Table 2]. Data are shown for the 15 CLM plant functional types: needleleaf evergreen tree (NET), needleleaf deciduous tree (NDT), broadleaf evergreen tree (BET), broadleaf deciduous tree (BDT), broadleaf evergreen shrub (BES), broadleaf deciduous shrub (BDS), C_3 and C_4 grass, and crop. Climate variants are: arctic (ar), boreal (bo), temperate (te), and tropical (tr).

fact, be significantly small, but its inclusion would necessitate new derivation of V_{cmax} from leaf gas exchange measurements [*Ethier and Livingston*, 2004]. The Rubisco kinetics and temperature dependence are from *Bernacchi et al.* [2001], as with *Kattge et al.* [2009] and *Medlyn et al.* [2002].

[12] The photosynthetic parameter J_{max}, which describes the maximum rate of electron transport, is typically specified from V_{cmax}. The ratio J_{max}/V_{cmax} depends on the Rubisco kinetics, and *Medlyn et al.* [2002] derived a value of 1.67 at 25°C using the *Bernacchi et al.* [2001] Rubisco parameters. This differs from the ratio 1.97 used in our model, derived by *Wullschleger* [1993] but with different Rubisco parameters, and we test model sensitivity to these values. We note, too, that the electron transport rate is specified through the same formulation as *Medlyn et al.* [2002], though parameter values differ. In the notation of *Bonan et al.* [2011], $\Theta_{PSII} = 0.7$ while *Medlyn et al.* [2002] used a value of 0.9. The quantum yield of electron transport is 0.3 mol electrons mol^{-1} photon in *Medlyn et al.* [2002], and our equivalent parameter is $I_{PSII} = 0.34$, assuming the same leaf absorptance of 0.8. However, *Medlyn et al.* [2002] noted that these two parameters only slightly affect J_{max} estimates.

2.3. Multilayer Canopy Model

[13] We hypothesize that CLM4 is too productive in the absence of nitrogen-reduced GPP because of deficiency in the two-leaf parameterization of radiative transfer and leaf photosynthesis and that the required nitrogen reduction compensates for the deficiency. Plant canopy models commonly parameterize leaf to canopy scaling using sunlit and shaded leaves and a vertical profile of photosynthetic capacity, specified through a within-canopy gradient of foliage nitrogen [*Leuning et al.*, 1995; *de Pury and Farquhar*, 1997; *Wang and Leuning*, 1998]. Our hypothesis is based on the observation that CLM4 and the revised model

of *Bonan et al.* [2011] both use a shallow gradient in nitrogen, lower than in some other models [*Bonan et al.*, 2011, Figure 3]). We test this hypothesis by devising a version of the model that explicitly resolves multilayer radiative transfer, leaf physiological traits, and photosynthesis for sunlit and shaded leaves at different depths in the canopy. Multilayer canopy models provide a reference solution for comparison with two-leaf canopy models [*de Pury and Farquhar*, 1997; *Wang and Leuning*, 1998], and we similarly use the multilayer canopy to diagnose inadequacy in the two-leaf canopy.

[14] The CLM4 uses the two-stream approximation to calculate radiative transfer of direct and diffuse radiation through a canopy that is differentiated into leaves that are sunlit and those that are shaded [*Oleson et al.*, 2010]. The two-stream equations are integrated over all plant area (leaf and stem area) in the canopy to calculate reflectance of solar radiation above the canopy (albedo), transmittance below the canopy onto the ground, and absorption by the canopy. The two-stream approximation provides a closed-form solution in contrast to more complex iterative multilayer radiation transfer schemes [e.g., *Norman*, 1979]. The CLM4 implementation of the two-stream approximation incorrectly diagnoses light absorption by the sunlit and shaded leaves, and *Bonan et al.* [2011] revised the model to correctly account for the sunlit and shaded fractions of the canopy in the context of the two-stream approximation. In the notation of *Bonan et al.* [2011], the absorption of direct beam radiation (per unit ground area) by the sunlit canopy is $\vec{I}^{\mu}_{sun,\Lambda}$ (their equation A7) and by the shaded canopy is $\vec{I}^{\mu}_{sha,\Lambda}$ (equation A8). For diffuse radiation, the absorption (per unit ground area) by the sunlit canopy is $\vec{I}_{sun,\Lambda}$ (equation A11) and by the shaded canopy is $\vec{I}_{sha,\Lambda}$ (equation A12). In this notation, the superscript μ denotes direct beam radiation; the subscripts *sun* and *sha* denote sunlit and shaded, respectively; and the subscript Λ denotes wave band (visible or near-infrared).

[15] In the multilayer canopy, we calculate canopy-integrated radiative fluxes as described in the preceding paragraph and additionally derive the light profile with depth in the canopy by taking the derivatives of the absorbed radiative fluxes with respect to cumulative plant area index (x). The terms $d\vec{I}^{\mu}_{sun,\Lambda}/dx$ and $d\vec{I}_{sun,\Lambda}/dx$ are the direct beam and diffuse solar radiation, respectively, absorbed by the sunlit fraction of the canopy (per unit plant area) at a depth defined by the cumulative plant area index x; $d\vec{I}^{\mu}_{sha,\Lambda}/dx$ and $d\vec{I}_{sha,\Lambda}/dx$ are the corresponding fluxes for the shaded fraction of the canopy at depth x. These fluxes are normalized by the sunlit or shaded fraction at depth x, defined by $f_{sun} = \exp(-K_b x)$, to give fluxes per unit sunlit or shaded plant area at depth x, with K_b the direct beam extinction coefficient (see Text S1 of the auxiliary material for details).[1] We compare the multilayer two-stream implementation with the multilayer radiative transfer theory of *Goudriaan* [1977] (see also *Goudriaan and van Laar* [1994]) and *Norman* [1979], implemented in many multilayer plant canopy models and considered here as benchmark reference code.

[16] For our global simulations, we resolve the canopy in increments of 0.25 m^2 m^{-2} and use the multilayer light profile to explicitly simulate photosynthesis and stomatal conductance for sunlit and shaded leaves at each layer in the canopy. The JULES model also calculates a light profile from the two-stream approximation but for larger leaf area increments [*Mercado et al.*, 2007; *Best et al.*, 2011]. The canopy energy balance and temperature are still calculated with the two-leaf approach, using in this case a canopy conductance derived from leaf stomatal conductance summed for the sunlit and shaded leaves in all canopy layers.

[17] Our multilayer model is only intended to address the nonlinearity of light profiles, photosynthesis, and stomatal conductance in the plant canopy. We compare the explicit calculation of photosynthesis at different levels in the canopy with the analytical two-leaf integration. We do not resolve profiles of temperature, humidity, wind, or CO_2 in the canopy, commonly represented in multilayer canopy models [*Goudriaan*, 1977; *Norman*, 1979; *Leuning et al.*, 1995; *Baldocchi and Wilson*, 2001; *Baldocchi et al.*, 2002; *Wohlfahrt et al.*, 2001; *Wohlfahrt*, 2004] but typically omitted in land surface schemes of global climate models. This is to ensure consistency between the two-leaf and multilayer canopy flux calculations. Total solar radiation absorbed by the canopy is the same in both approaches, and the multilayer model additionally resolves the profile of that absorbed radiation.

[18] Canopy models commonly decrease leaf photosynthetic capacity with depth in the canopy using an exponential profile of foliage nitrogen [*Leuning et al.*, 1995; *de Pury and Farquhar*, 1997; *Wang and Leuning*, 1998]. The CLM4 uses a comparable approach, but the gradient in foliage nitrogen is specified through a linear increase in specific leaf area with greater depth in the canopy. *Bonan et al.* [2011] revised the model to use the exponential profile. In the two-leaf and multilayer models, $V_{c\max}$ is specified at the canopy top and is scaled with depth using the function

$$V_{c\max}(x) = V_{c\max}(0)\exp(-K_n x), \tag{1}$$

where here x is cumulative leaf area index and $K_n = 0.11$, so that $V_{c\max}$ at the canopy top, denoted by $V_{c\max}(0)$, decreases exponentially with greater cumulative leaf area (equation C4 in *Bonan et al.* [2011]). The maximum electron transport rate ($J_{\max}$), leaf respiration rate, and other photosynthetic parameters are specified from $V_{c\max}$ (at 25°C) at the canopy top and are similarly scaled with canopy depth [*Bonan et al.*, 2011, Tables B3 and B4]. The two-leaf canopy uses canopy-integrated values [*Bonan et al.*, 2011, equations C4–C8]. The multilayer canopy explicitly resolves these parameters at each layer using the exponential profile given by (1).

[19] The value $K_n = 0.11$ chosen by *Bonan et al.* [2011] is consistent with observationally derived estimates for forests, mostly tropical, and provides a gradient in $V_{c\max}$ similar to the original CLM4 specific leaf area scaling. In more recent work, *Lloyd et al.* [2010] analyzed numerous forest canopies and found that K_n scales with $V_{c\max}$ with the relationship

$$K_n = \exp(0.00963 V_{c\max} - 2.43) \tag{2}$$

such that higher values of $V_{c\max}$ imply steeper declines in photosynthetic capacity through the canopy with respect to

[1] Auxiliary materials are available in the HTML. doi:10.1029/2011JG001913.

Table 1. Model Simulations

Simulation	Canopy	$V_{c\max}$	K_n	$J_{\max}$	Description
2Lnit	two-leaf	nitrogen-reduced	0.11	1.97 $V_{c\max}$	control simulation
2Lpot	two-leaf	potential	0.11	1.97 $V_{c\max}$	potential $V_{c\max}$ without nitrogen reduction
2Lobs	two-leaf	*Kattge et al.* [2009]	0.11	1.97 $V_{c\max}$	observed $V_{c\max}$ in the environment
2LobsKn3	two-leaf	*Kattge et al.* [2009]	0.30	1.97 $V_{c\max}$	sensitivity to K_n
2LobsKn5	two-leaf	*Kattge et al.* [2009]	0.50	1.97 $V_{c\max}$	sensitivity to K_n
MLobs	multilayer	*Kattge et al.* [2009]	0.11	1.97 $V_{c\max}$	multilayer canopy radiation with observed $V_{c\max}$; compare with 2Lobs
MLkn	multilayer	*Kattge et al.* [2009]	*Lloyd et al.* [2010]	1.97 $V_{c\max}$	K_n depends on $V_{c\max}$
MLjmx	multilayer	*Kattge et al.* [2009]	*Lloyd et al.* [2010]	*Medlyn et al.* [2002]	$J_{\max} = 1.67\ V_{c\max}$

cumulative leaf area. This new data provides an additional observational constraint on leaf to canopy scaling. With the *Kattge et al.* [2009] values (Figure 1) applied to the canopy top, K_n varies from 0.13 to 0.23. We test model sensitivity to a uniform $K_n = 0.11$ and to K_n determined from $V_{c\max}$. In the latter case, we specify K_n from $V_{c\max}$ (at 25°C) at the canopy top.

[20] The parameter $J_{\max}$ is an important constraint on leaf photosynthesis. The ratio of $J_{\max}$ to $V_{c\max}$ determines the irradiance at which leaf photosynthesis is Rubisco-limited or light-limited [*Wang*, 2000]. The value of $J_{\max}$ at 25°C can be determined by the corresponding value of $V_{c\max}$, but there is uncertainty in this ratio and it varies with the particular form of the photosynthesis model [*Medlyn et al.*, 2002; *Kattge and Knorr*, 2007]. *Bonan et al.* [2011] use a ratio of 1.97, from *Wullschleger* [1993], which is similar to the value of 2.00 reported by *Leuning* [2002], but *Medlyn et al.* [2002] found that

$$J_{\max} = 1.67 V_{c\max} \tag{3}$$

at 25°C. This alters the light level (and therefore the depth in the canopy) at which photosynthesis is light-limited rather than Rubisco-limited. The *Medlyn et al.* [2002] estimate is more consistent with our photosynthesis model than is the *Wullschleger* [1993] estimate. We test the sensitivity of the multilayer model to specification of $J_{\max}$ using the ratios 1.97 and 1.67.

2.4. Model Simulations

[21] Simulations followed the protocol of *Bonan et al.* [2011] and used: prescribed satellite-derived monthly leaf area index without the CLM4CN carbon-nitrogen biogeochemistry; a 57-year (1948–2004) meteorological data set to force the model; constant land cover for the year 2000; yearly atmospheric CO_2 from the historical record; and a spatial resolution of 1.25 degrees in longitude by 0.9375 degrees in latitude.

[22] When calculating leaf surface humidity for the Ball-Berry stomatal conductance model, CLM4 has a lower limit to canopy air vapor pressure to prevent numerical instability at low humidity. The simulations of *Bonan et al.* [2011] retained this lower limit (25% relative humidity for C_3 plants and 40% for C_4 plants; see equations in their Table B1). However, their revised photosynthesis-conductance equations do not have similar numerical instability, and here we set this limit to a small value (5% relative humidity). The effect on simulated GPP is minor, and all simulations described hereafter used this revision.

[23] We performed eight simulations to document differences between the standard two-leaf canopy and the multilayer canopy (Table 1). The first three simulations used the two-leaf canopy and examined model sensitivity to $V_{c\max}$: 2Lnit, a control simulation using the nitrogen-reduced values for $V_{c\max}$; 2Lpot, a simulation using the potential values for $V_{c\max}$ before nitrogen reduction; and 2Lobs, a simulation with $V_{c\max}$ set to the values of *Kattge et al.* [2009]. *Kattge et al.* [2009] did not provide a value for C_4 grass, and we used the CLM4 potential value (52 μmol CO_2 m^{-2} s^{-1}) for C_4 plants, so that $V_{c\max}$ was unchanged for C_4 grass between the 2Lpot and 2Lobs simulations. (The same simulation reported in *Bonan et al.* [2011] used 78 μmol CO_2 m^{-2} s^{-1}, which was too large.) *Bonan et al.* [2011] performed three similar simulations, but in contrast, the simulations herein used the lower C_4 $V_{c\max}$, the revised canopy air vapor pressure threshold, and are reported here again for clarity.

[24] Some two-leaf canopy models use higher values for K_n than in the simulations herein (e.g., $K_n \sim 0.5$). Two additional simulations examined the sensitivity of the two-leaf canopy to K_n. We repeated the 2Lobs simulation with $K_n = 0.3$ (2LobsKn3) and $K_n = 0.5$ (2LobsKn5) to ask if larger values of K_n match results for the multilayer canopy.

[25] Three other simulations examined the multilayer canopy model: MLobs is the multilayer radiative transfer with *Kattge et al.* [2009] $V_{c\max}$ (compare with 2Lobs using $K_n = 0.11$); MLkn, as in MLobs but additionally with the *Lloyd et al.* [2010] dependence of the canopy scaling coefficient K_n on $V_{c\max}$ (from equation 2); and MLjmx, as in MLkn but additionally with the *Medlyn et al.* [2002] dependence of $J_{\max}$ on $V_{c\max}$ (from equation 3).

2.5. FLUXNET Data

[26] We compared the model simulations to FLUXNET GPP and latent heat flux estimates. We used upscaled annual GPP and latent heat flux, as in *Bonan et al.* [2011]. As an additional test, we also compared the model simulations with GPP light-response curves for individual FLUXNET tower sites.

[27] Data-oriented diagnostic techniques have been used to upscale GPP and latent heat flux from the FLUXNET network of tower sites to global 0.5° gridded data [*Jung et al.*, 2010, 2011; *Beer et al.*, 2010]. The upscaling relies on remotely sensed estimates of the fraction of absorbed photosynthetically active radiation, climate, and land cover and provides monthly fluxes at 0.5° spatial resolution. We

Table 2. FLUXNET Sites Used for Light-Response Curves in This Study[a]

				FLUXNET			LAI	
Site	Lat. (°N)	Lon. (°E)	Climate Zone	Years	*n*	Model *n*	FLUXNET	Model
			ENF					
CA-NS2	55.9	−98.5	Boreal	2001–2005	63	42	8	4
CA-Obs	54.0	−105.1	Boreal	1999–2005	104	42	4	5
CA-Ojp	53.9	−104.7	Boreal	1999–2005	90	42	3	5
CA-Qfo	49.7	−74.3	Boreal	2003–2006	56	42	4	5
U.S.-Ho1	45.2	−68.7	Humid continental, cool summer	1996–2004	131	42	6	6
U.S.-Me4	44.5	−121.6	Subtropical-Mediterranean	1996–2000	40	24	2	4
CA-Ca1	49.9	−125.3	Marine	1997–2005	74	41	8	4
U.S.-Dk3	36.0	−79.1	Humid subtropical	2001–2005	59	42	5	6
			DBF					
CA-Oas	53.6	−106.2	Boreal	1997–2005	138	42	2	3
U.S.-WCr	45.8	−90.1	Humid continental, cool summer	1999–2006	58	42	5	6
U.S.-UMB	45.6	−84.7	Humid continental, cool summer	1999–2003	73	42	4	5
U.S.-Ha1	42.5	−72.2	Humid continental, cool summer	1991–2006	140	42	5	6
U.S.-MMS	39.3	−86.4	Humid subtropical	1999–2005	89	42	5	5
U.S.-Dk2	36.0	−79.1	Humid subtropical	2004–2005	14	42	6	6
			EBF					
BR-Ma2	−2.6	−60.2	Tropical	1999, 2000, 2002–2006	73	42	5	5
BR-Sa1	−2.9	−55.0	Tropical	2002–2004	43	42	5	5
BR-Sa3	−3.0	−55.0	Tropical	2000–2003	45	42	5	5
BR-Ji2	−10.1	−61.9	Tropical	2000–2002	28	37	5	6
			GRA					
CA-Let	49.7	−112.9	Humid continental, cool summer	1998–2005	118	34	-	2
U.S.-FPe	48.3	−105.1	Semi-arid	2000–2006	63	30	2	2
U.S.-Bkg	44.3	−96.8	Humid continental, warm summer	2004–2006	39	41	3	2
U.S.-ARc	35.5	−98.0	Humid subtropical	2005–2006	31	26	2	2
			CRO					
U.S.-IB1	41.9	−88.2	Humid continental, warm summer	2005–2007	28	42	1–3	2
U.S.-Bo1	40.0	−88.3	Humid continental, warm summer	1996–2007	129	42	-	2
U.S.-Bo2	40.0	−88.3	Humid continental, warm summer	2004–2006	37	42	-	2
U.S.-Ne3	41.2	−96.4	Humid continental, warm summer	2001–2005	57	37	1–4	2

[a]Biome types: evergreen needleleaf forest (ENF), deciduous broadleaf forest (DBF), evergreen broadleaf forest (EBF), grassland (GRA), cropland (CRO). The years of data and number of light-response curves analyzed (*n*) are shown for FLUXNET. Model simulations were analyzed for years 2002–2004, and shown are the number of model light-response curves (*n*) for each site. Leaf area index (LAI) is the maximum reported in the FLUXNET 'La Thuile' database (http://www.fluxdata.org), or for cropland is the range of values for July. Model leaf area index also includes stem area (about 1 m^2 m^{-2} for forests, 0.5 for grassland, and 0.1 for cropland).

compared the model simulations with the annual upscaled GPP and latent heat flux for the 23-year period 1982–2004, as in *Bonan et al.* [2011].

[28] We used the empirical models of *Lasslop et al.* [2010] as estimates of the observed light-response curves at individual flux tower sites. *Lasslop et al.* [2010] used half hourly eddy covariance measurements of net ecosystem exchange (NEE) from the FLUXNET 'La Thuile' database (http://www.fluxdata.org) and fit the light-response curve

$$NEE = \frac{\alpha\beta R_g}{\alpha R_g + \beta} + \gamma, \tag{4}$$

where α (μmol CO_2 J^{-1}) is the canopy light use efficiency and represents the initial slope of the light-response curve, β (μmol CO_2 m^{-2} s^{-1}) is the maximum uptake rate of the canopy at light saturation, R_g (W m^{-2}) is the global radiation, and γ (μmol CO_2 m^{-2} s^{-1}) is the ecosystem respiration. The parameter β is defined as

$$\beta = \begin{cases} \beta_0 \exp\left[-k(D - D_0)\right], & D > D_0 \\ \beta_0, & D < D_0 \end{cases}, \tag{5}$$

where D (hPa) is vapor pressure deficit, D_0 = 10 hPa is the threshold vapor pressure deficit, and k (hPa^{-1}) is an empirical parameter. *Lasslop et al.* [2010] modeled respiration as a function of temperature according to *Lloyd and Taylor* [1994] with a base respiration at 15°C (r_b) and a temperature sensitivity parameter (E_0). *Lasslop et al.* [2010] estimated the parameters α, β_0, k, and r_b every two days with a 4-day moving window to accommodate temporal variability not included in the equations; E_0 was estimated separately using nighttime data.

[29] We used light-response curves for 26 FLUXNET sites covering a range of boreal, temperate, and tropical climates and forest, grassland, and cropland vegetation (Table 2). The forests sites are generally closed canopy with leaf area index of 4–6 m^2 m^{-2}, though CA-Ojp, U.S.-Me4, and CA-Oas have more open canopies with lower leaf area. The grassland and cropland sites are sparse canopies with lower leaf area index (2–3 m^2 m^{-2}). For our analysis, we used the *Lasslop et al.* [2010] estimates for α and β_0 and calculated GPP as

$$GPP = \frac{\alpha\beta_0 R_g}{\alpha R_g + \beta_0} \tag{6}$$

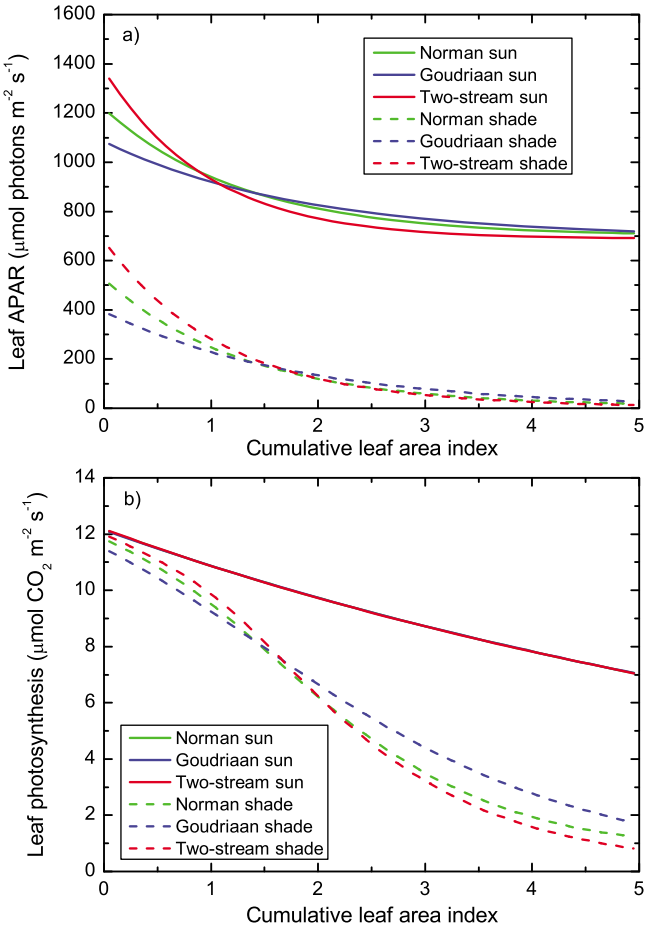

Figure 2. Profiles of (a) absorbed photosynthetically active radiation (APAR) and (b) photosynthesis for sunlit and shaded leaves in relation to cumulative leaf area index in a canopy. Fluxes are per unit leaf area. Shown are simulations using the two-stream approximation and the radiative transfer theory of *Goudriaan* [1977] and *Norman* [1979]. The leaf photosynthesis model is as described by *Bonan et al.* [2011], using leaf parameter values at 25°C. The simulations are for a canopy with cumulative leaf area index 5 m^2 m^{-2}, spherical leaf angle distribution, and zenith angle 30°. Incident photosynthetic photon flux density at the top of the canopy is 2000 μmol m^{-2} s^{-1}, and the diffuse fraction is 0.3. Leaf reflectance and transmittance are 0.10 and 0.05, respectively, and soil albedo is 0.1. V_{cmax} and J_{max} at the top of the canopy are 60 and 118.2 μmol m^{-2} s^{-1}, respectively, and leaf traits scale with canopy depth using the coefficient K_n = 0.11. In these simulations, c_i = 266 μmol mol^{-1} ($0.7c_a$). The canopy is resolved in leaf area increments of 0.1 m^2 m^{-2}.

to represent maximum GPP in the absence of vapor pressure deficit limitation. In this equation, β_0/α defines R_g at which $GPP = 0.5\beta_0$.

[30] We analyzed monthly light-response curves for these sites during the main growing season. For tropical evergreen broadleaf forest, we used light-response curves for the month of March, during the wet season. For all the other sites, we used the month of July to represent the Northern Hemisphere growing season. The observed light-response curves for each site spanned several years of data, with temporally varying α and β_0 within a month and between years. We created a statistical composite (mean, median, first quartile, and third quartile) of all the light-response curves for various dates in the month and for all years. The number of light-response curves at each site was generally 30 or more, except U.S.-Dk2 with only 14 individual curves (Table 2).

[31] In order to generate quantities that are directly comparable between the model and the observations, we fit half hourly GPP from the model simulations to the light-response curve (6). We used model data for the months of March (tropical evergreen broadleaf forest) or July (all other sites) and for the years 2002–2004. These years overlap with the FLUXNET data at most sites. We sampled only the half hourly data with relative humidity greater than 75%, to exclude vapor pressure deficit limitation as in (6), and additionally for cropland restricted air temperature to less than 300 K (26.85°C) to eliminate high temperatures. Model data was obtained for the grid cell co-located with the FLUXNET tower site. For some tower sites, the same model grid cell represented two sites (CA-Obs and CA-Ojp; BR-Sa1 and BR-Sa3; U.S.-Bo1 and U.S.-Bo2). Model grid cells represent a mosaic of individual vegetation tiles; we sampled GPP from the plant functional type representative of the FLUXNET tower site. Tree tiles were similar to the FLUXNET tower sites, generally closed canopy with leaf area index of 4–6 m^2 m^{-2} (Table 2). Grassland and cropland were more sparse canopies with leaf area index of 2 m^2 m^{-2}.

[32] The parameters α and β_0 for (6) were estimated from model data every two days with a 4-day moving window using the Levenberg-Marquardt algorithm, as in *Lasslop et al.* [2010]. This generally produced 42 individual curves (14 for a month × 3 years), though some sites had less due to the sampling restrictions (Table 2). We compared FLUXNET and model light-response curves in their statistics (mean, median, first quartile, and third quartile) and also in mean light use efficiency (α) and mean photosynthetic capacity. Photosynthetic capacity was defined as GPP calculated from (6) with R_g = 870 W m^{-2} (a photosynthetic photon flux density of 2000 μmol m^{-2} s^{-1}) and denoted GPP_{2000}.

3. Results

3.1. Radiative Transfer

[33] The absorbed light profile simulated with the two-stream approximation is consistent with the multilayer radiative transfer models of *Goudriaan* [1977] and *Norman* [1979], though the two-stream approximation has higher absorbed photosynthetically active radiation for leaves at the top of the canopy (Figure 2a). Leaf photosynthesis simulated with these light profiles is similar among radiative transfer parameterizations (Figure 2b). Photosynthesis for sunlit leaves is virtually identically for the three radiative parameterizations. Differences are larger for shaded leaf photosynthesis, especially near the canopy bottom.

[34] With K_n = 0.11 and with only beam radiation incident on the canopy (i.e., diffuse fraction of incident radiation is zero, f_d = 0), the response of canopy photosynthesis to light intensity is similar for the three multilayer radiative transfer parameterizations (Figure 3a, solid lines). The Norman and Goudriaan solutions are indistinguishable, while the two-

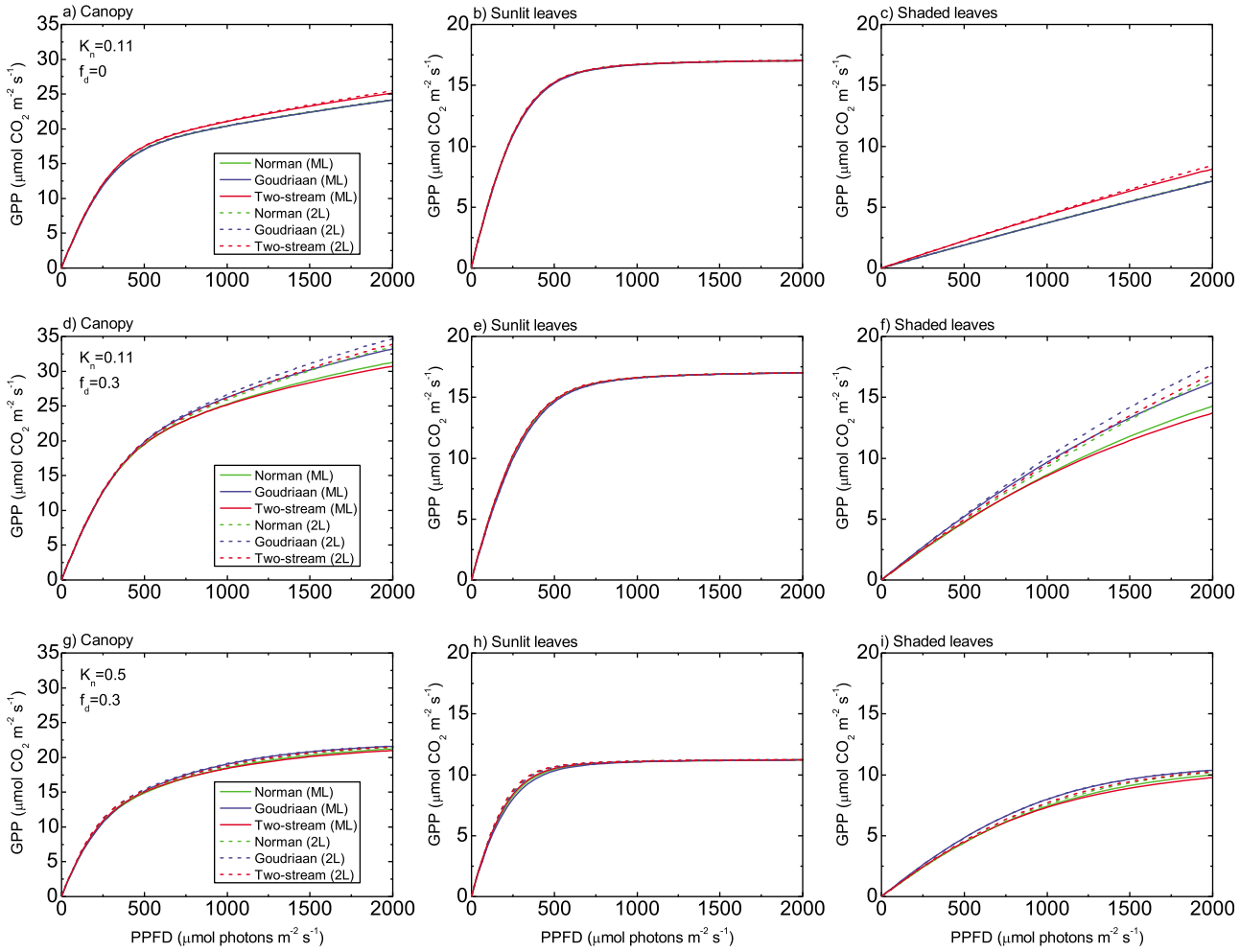

Figure 3. Photosynthesis in relation to incident light at the top of the canopy (PPFD, photosynthetic photon flux density) simulated with the two-stream, *Goudriaan* [1977], and *Norman* [1979] radiative transfer models. Shown are fluxes (per unit ground area) for the total canopy (Figures 3a, 3d, and 3g), the sunlit canopy (Figures 3b, 3e, and 3h), and the shaded canopy (Figures 3c, 3f, and 3i). Each panel shows solutions for the three multilayer canopies (solid lines) and the corresponding solution for a two-leaf canopy (dashed lines). Simulations are as in Figure 2. Results are shown for (a–c) $K_n = 0.11$ and diffuse fraction $f_d = 0$, (d–f) $K_n = 0.11$ and $f_d = 0.3$, and (g–i) $K_n = 0.5$ and $f_d = 0.3$.

stream radiation produces slightly higher photosynthesis. The light-response can be compared to a comparable two-leaf canopy (representing a sunlit and a shaded leaf) for each of the three radiative transfer parameterizations (Figure 3a, dashed lines). The two-leaf canopy uses the light absorption for the average sunlit and shaded leaf to calculate photosynthesis. Using the same parameter values ($K_n = 0.11$ and $f_d = 0$), the multilayer and two-leaf canopies are indistinguishable. Similar results are seen for sunlit leaves (Figure 3b) and shaded leaves (Figure 3c).

[35] When f_d increases to 0.3 ($K_n = 0.11$ as before), the multilayer canopy results in lower canopy photosynthesis at high irradiance than the comparable two-leaf canopy for each of the three radiative transfer parameterizations (Figure 3d), even though total radiation absorption is similar in the multilayer and two-leaf canopies (not shown). Sunlit leaf photosynthesis does not vary among models (Figure 3e). The difference between the multilayer and two-leaf canopies arises in shaded leaves (Figure 3f) and results from the averaging of light absorption over the shaded leaves (as applied on the nonlinear photosynthetic equations). The difference increases with higher irradiance, is largest for the two-stream radiation, and is least for the Goudriaan radiation.

[36] With larger K_n, the difference between the two-leaf and multilayer canopies decreases ($f_d = 0.3$ and $K_n = 0.5$, Figures 3g–3i). The Goudriaan radiation is virtually identical between the two canopies. The Norman and two-stream parameterizations have slightly larger differences between canopies, particularly for shaded leaves.

3.2. Annual GPP and Evapotranspiration

[37] *Jung et al.* [2011] estimated global annual GPP to be 119 ± 6 Pg C yr^{-1} based on FLUXNET data for the period 1982–2008. *Beer et al.* [2010] obtained 123 ± 8 Pg C yr^{-1} for the period 1998–2005 based on a multimodel ensemble analysis of FLUXNET data. The FLUXNET-derived global

Table 3. Global GPP and Evapotranspiration From Model Simulations for Years 1982–2004

Simulation	GPP (Pg C yr^{-1})	Evapotranspiration (10^3 km^3 yr^{-1})
2Lnit	129	65
2Lpot	161	67
2Lobs	161	67
2LobsKn3	146	66
2LobsKn5	132	64
MLobs	147	65
MLkn	144	65
MLjmx	138	65

annual evapotranspiration is estimated to be $65 \pm 3 \times 10^3$ km^3 yr^{-1} [*Jung et al.*, 2011]. Our simulations extended over the period 1982–2004. The 2Lnit simulation is consistent with these estimates, while the 2Lpot and 2Lobs simulations overestimate GPP and evapotranspiration (Table 3), as previously reported by *Bonan et al.* [2011]. The multilayer model reduces these biases (MLobs, MLkn, MLjmx, Table 3).

[38] The annual GPP biases have a distinct geographic pattern, shown in Figure 4 as zonal averages for the simulations and for the FLUXNET data. The high V_{cmax} in the 2Lpot simulation yields large GPP that exceeds the FLUXNET data at all latitudes (Figure 4a). The 2Lnit simulation with reduced V_{cmax} decreases GPP compared with 2Lpot and replicates the FLUXNET data quite well in the extratropics, but overestimates GPP in the tropics. The 2Lobs simulation with observed V_{cmax} more closely matches FLUXNET data in the tropics, where V_{cmax} for tropical broadleaf evergreen trees is considerably lower than that used in 2Lpot and 2Lnit. Annual GPP in the 2Lobs simulation exceeds that of the 2Lpot simulation in middle latitudes (30–60° N), where V_{cmax} for broadleaf deciduous and needleleaf evergreen trees (temperate and boreal), C_3 grass, and crop is higher than that in 2Lpot. The multilayer model reduces annual GPP compared with the 2Lobs simulation (Figure 4b) and better matches FLUXNET data, though results are still biased high in the extratropics.

[39] The 2Lobs simulation overestimates annual GPP in boreal regions of North America and Eurasia, in temperate regions of North America and Europe, and savannas of South America and Africa (Figure 5a). The multilayer radiation (MLobs) reduces these biases (Figure 5b), and the MLkn and MLjmx simulations further reduce the biases (Figures 5c and 5d). The greatest reduction in GPP comes from the multilayer radiation (MLobs). Lower J_{max} (MLjmx) has the second largest effect. Dependence of K_n on V_{cmax} (MLkn) yields the smallest reduction in GPP. Root mean square error of GPP is reduced in the multilayer simulations compared with the 2Lobs simulation and is comparable to the 2Lnit simulation (Table 4).

[40] Table 5 shows model simulations averaged for various biomes. In temperate and boreal forest, the increase in GPP due to observed V_{cmax} (2Lobs - 2Lnit) is greatly offset by the multilayer radiation (MLobs - 2Lobs) and variable K_n (MLkn - MLobs). The net GPP increase (MLkn - 2Lnit) is small relative to 2Lnit in temperate forest (146 g C m^{-2} yr^{-1}, 9%) and boreal forest (134 g C m^{-2} yr^{-1}, 13%). Decreased J_{max} (MLjmx - MLkn) produces further reduction in GPP so that the higher GPP from observed V_{cmax} is largely offset. The multilayer model has less effect in grassland, cropland, and tundra, where the dominant response is an increase in GPP due to observed V_{cmax}. Similarly, annual GPP in tropical

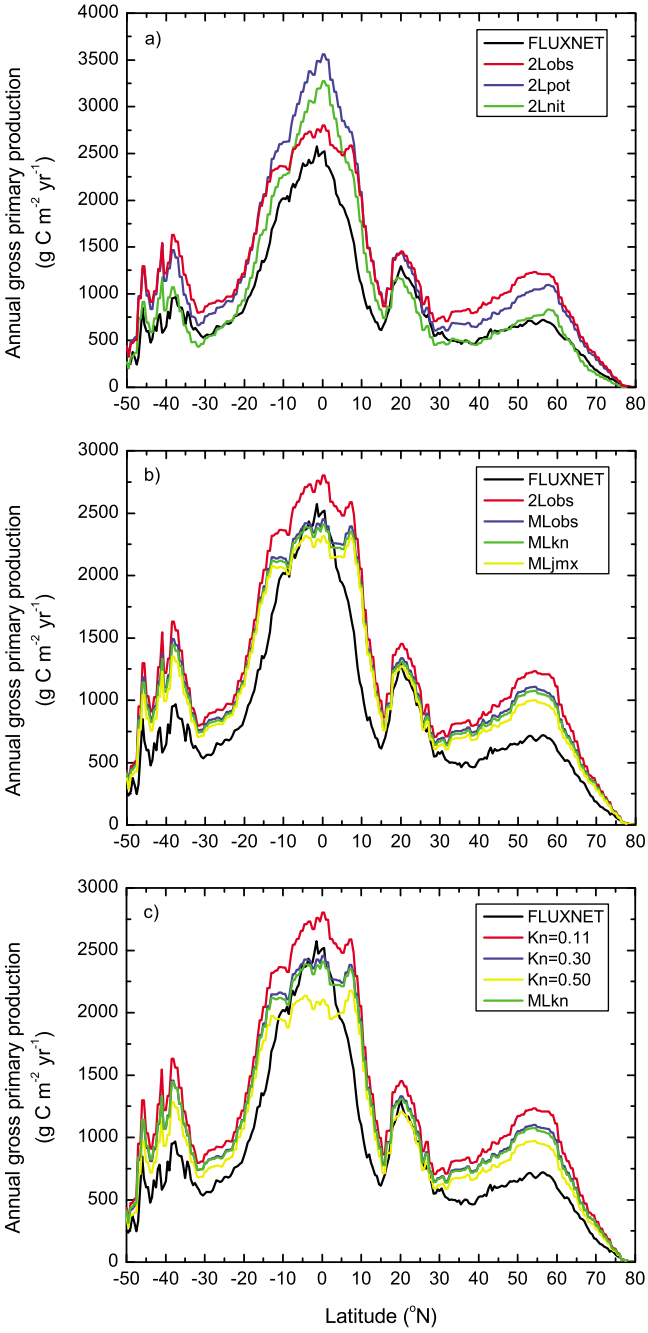

Figure 4. Zonal average annual GPP (1982–2004) for model simulations compared with FLUXNET estimates. (a) Simulations for the two-leaf canopy with observed V_{cmax} (2Lobs), the CLM4 potential values (2Lpot), and the CLM4 nitrogen-reduced values (2Lnit). (b) The 2Lobs simulation compared with multilayer canopy simulations using observed V_{cmax} and radiation only (MLobs), radiation and K_n (MLkn), and radiation, K_n, and J_{max} (MLjmx). (c) The 2Lobs simulation (K_n = 0.11), additional two-leaf simulations with K_n = 0.30 and 0.50, and MLkn.

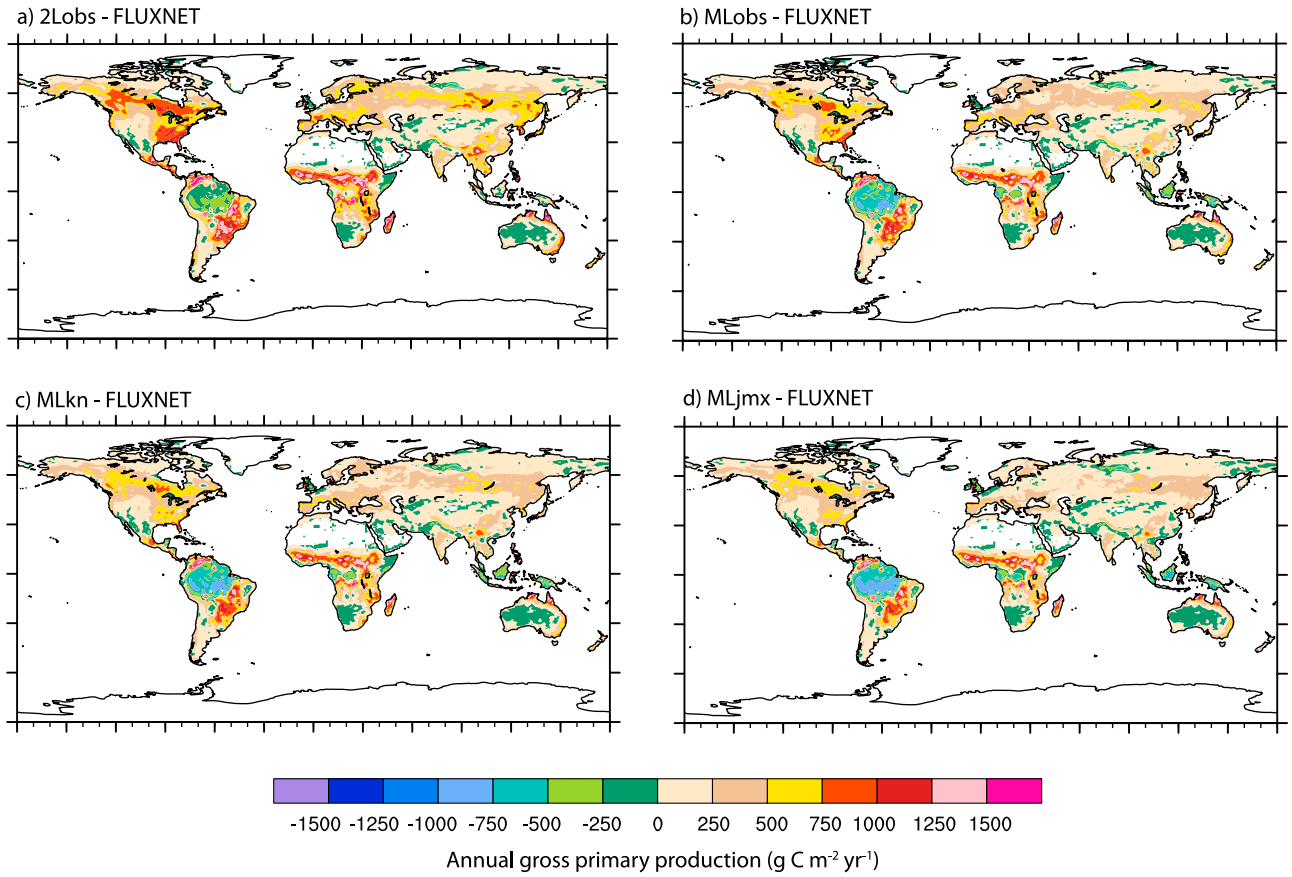

Figure 5. Annual GPP (1982–2004) compared with FLUXNET estimates for (a) the two-leaf canopy using observed V_{cmax} (2Lobs) and for the multilayer canopy using observed V_{cmax} with (b) radiation only (MLobs), (c) radiation and K_n (MLkn), and (d) radiation, K_n, and J_{max} (MLjmx).

evergreen forest declines greatly with observed V_{cmax}, and this decline is accentuated with the multilayer model.

[41] Figure 6 summarizes the main result of the simulations. The two-leaf model is biased high compared with FLUXNET GPP when V_{cmax} is not reduced for nitrogen availability (2Lpot). This bias decreases with nitrogen-reduced V_{cmax} (2Lnit), and the model closely matches FLUXNET except in the tropics. Observed V_{cmax} (2Lobs) increases GPP and the two-leaf model is biased high compared with FLUXNET, with the prominent exception of the Amazonia region of South America. The multilayer canopy (MLkn) reduces GPP and therefore reduces these biases (with the exception of Amazonia). Biases in the MLkn simulation are comparable to, though of opposite sign, those of the 2Lnit simulation. Negative biases of 0 to −250 g C m^{-2} yr^{-1} in tundra regions in 2Lnit are replaced by positive biases of 0 to 250 g C m^{-2} yr^{-1} in MLkn. Negative biases of −250 to −500 g C m^{-2} yr^{-1} in central United States and central Europe in 2Lnit are replaced by positive biases of 250 to 500 g C m^{-2} yr^{-1} in MLkn. Large biases in tropical Africa and Indonesia in 2Lnit are greatly improved in MLkn, with the prominent exception of South America.

[42] Some improvements are also seen in latent heat flux (Figure 7). Annual latent heat flux in the 2Lnit simulation is biased low throughout much of the Northern Hemisphere middle and high latitudes. The multilayer canopy (MLkn) increases latent heat flux and reduces these biases. However, the multilayer canopy decreases latent heat flux in the tropics and increases the negative biases. Root mean square error is unchanged among simulations (Table 4).

[43] When K_n is set to high values, the 2Lobs simulation is similar to the multilayer canopy simulations. This is seen in global annual GPP and evapotranspiration (Table 3) and also zonal GPP (Figure 4c). The 2LobsKn3 simulation (K_n = 0.3) reduces GPP compared with 2Lobs (K_n = 0.11), reduces biases compared with FLUXNET, and is similar to the MLkn simulation. The 2LobsKn5 simulation (K_n = 0.5) further reduces GPP, but introduces a low bias in the tropics.

3.3. Canopy Light-Response Curves

[44] Figures 8 and 9 show observed and simulated light-response curves for representative tower sites. Clearest results are for boreal evergreen needleleaf forest, illustrated in Figure 8a for CA-Qfo. The 2Lnit simulation overestimates GPP at all light levels compared with the FLUXNET data

Table 4. Root Mean Square Error of Model Simulations[a]

Metric	2Lnit	2Lobs	MLkn	MLjmx
GPP (g C m^{-2} yr^{-1})	400	552	453	431
Latent heat flux (W m^{-2})	13	13	13	13

[a]GPP and latent heat flux are the root-mean-square error compared with FLUXNET upscaled fields for each model grid cell. Data are averaged for years 1982–2004.

Table 5. Annual GPP (g C m^{-2} yr^{-1}) by Biome for the Control Simulation and Model Changes[a]

Effect	Simulation	Tropical Evergreen Forest	Temperate Forest	Boreal Forest	Grassland	Cropland	Tundra
Control	2Lnit	3640	1679	1032	463	417	152
V_{cmax}	2Lobs - 2Lnit	−717	470	353	150	622	196
ML radiation	MLobs - 2Lobs	−420	−269	−187	−20	−31	−28
K_n	MLkn - MLobs	−34	−55	−32	−5	−36	−6
Subtotal	MLkn - 2Lnit	−1171	146	134	125	555	162
J_{max}	MLjmx - MLkn	−99	−108	−80	−7	−56	−19
Total	MLjmx - 2Lnit	−1270	38	54	118	499	143

[a]Biomes are defined based on dominant plant functional type. Cropland is restricted to North America and tundra is north of 60°N. Simulations are averaged for years 1982–2004.

for CA-Qfo. Higher observed V_{cmax} in the 2Lobs simulation increases GPP and yields a poorer simulated light-response curve. The multilayer canopy (MLkn and MLjmx) decreases GPP and improves the light-response curve compared with 2Lobs. Similar results are found at the other three boreal evergreen needleleaf forest sites (CA-NS2, CA-Obs, and CA-Ojp, Figure S1 of the auxiliary material), and summarized for all four sites in Figure 10 in terms of root mean square error (RMSE), photosynthetic capacity (GPP_{2000}), and light use efficiency (α). Across boreal evergreen needleleaf forest sites, the 2Lobs simulation has increased RMSE and high GPP_{2000} compared with 2Lnit. The MLkn simulation decreases RMSE and GPP_{2000} compared with 2Lobs. The MLjmx simulation has additional improvement.

[45] Results for temperate evergreen needleleaf forests are mixed (Figure S2 of the auxiliary material). There is small difference in V_{cmax} between the 2Lnit and 2Lobs simulations. Both simulations produce light-response curves consistent with FLUXNET with low RMSE and small bias in GPP_{2000} (Figure 10). Observed V_{cmax} degrades the 2Lobs simulation at U.S.-Me4, where GPP_{2000} is biased high. The MLkn simulation has improved RMSE and GPP_{2000} relative to 2Lobs at U.S.-Me4, but increased error at the other three sites. Overall, RMSE and GPP_{2000} degrade in MLkn relative to 2Lobs (Figure 10). The MLjmx simulation reinforces these effects.

[46] For deciduous broadleaf forest, the 2Lnit simulation underestimates GPP at high light compared with FLUXNET

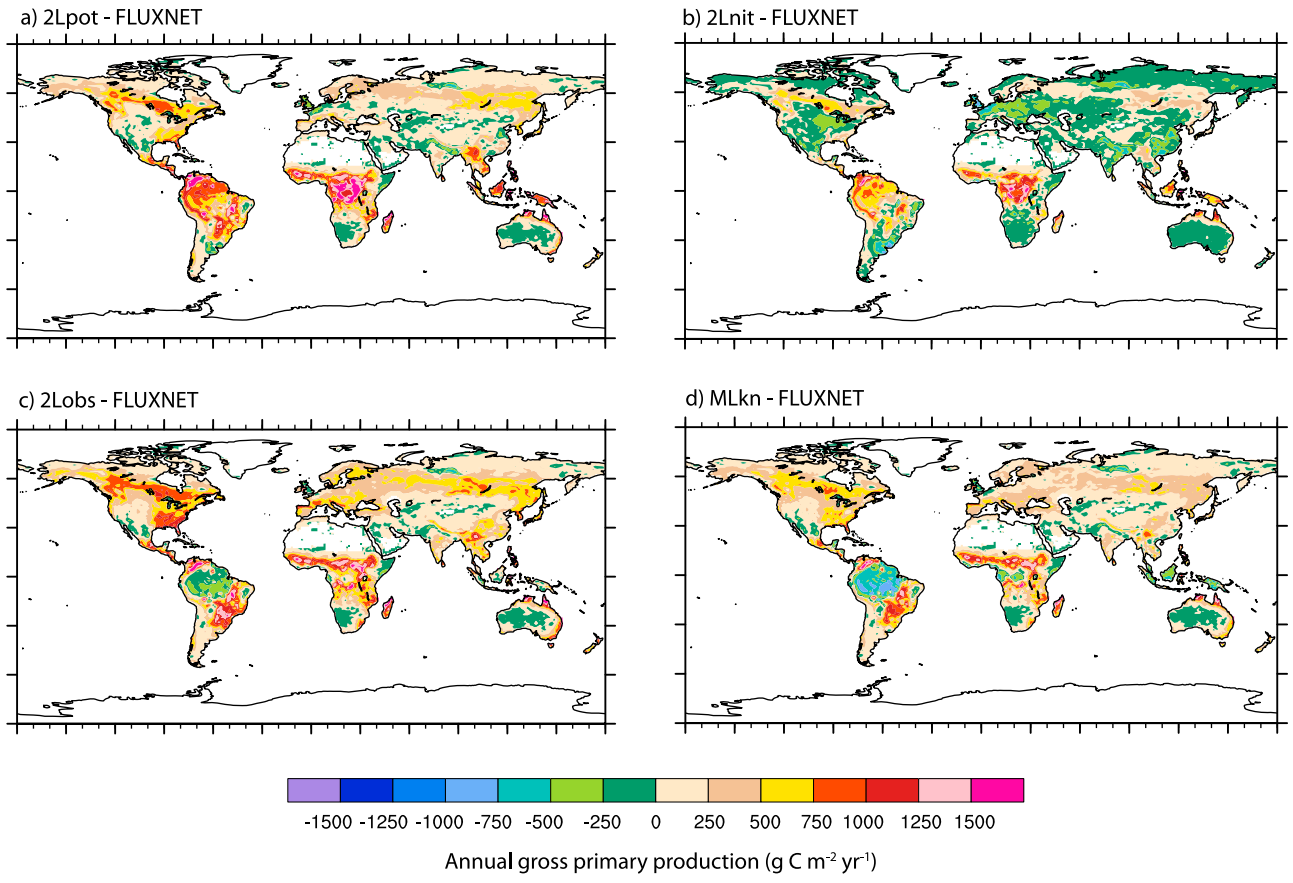

Figure 6. Annual GPP (1982–2004) for model simulations compared with FLUXNET estimates. (a) Annual GPP for the 2Lpot simulation without nitrogen-reduced V_{cmax}, and (b) the corresponding 2Lnit simulation with nitrogen-reduced V_{cmax}. (c) Annual GPP for the 2Lobs simulation with observed V_{cmax}, and (d) the corresponding MLkn simulation for the multilayer canopy.

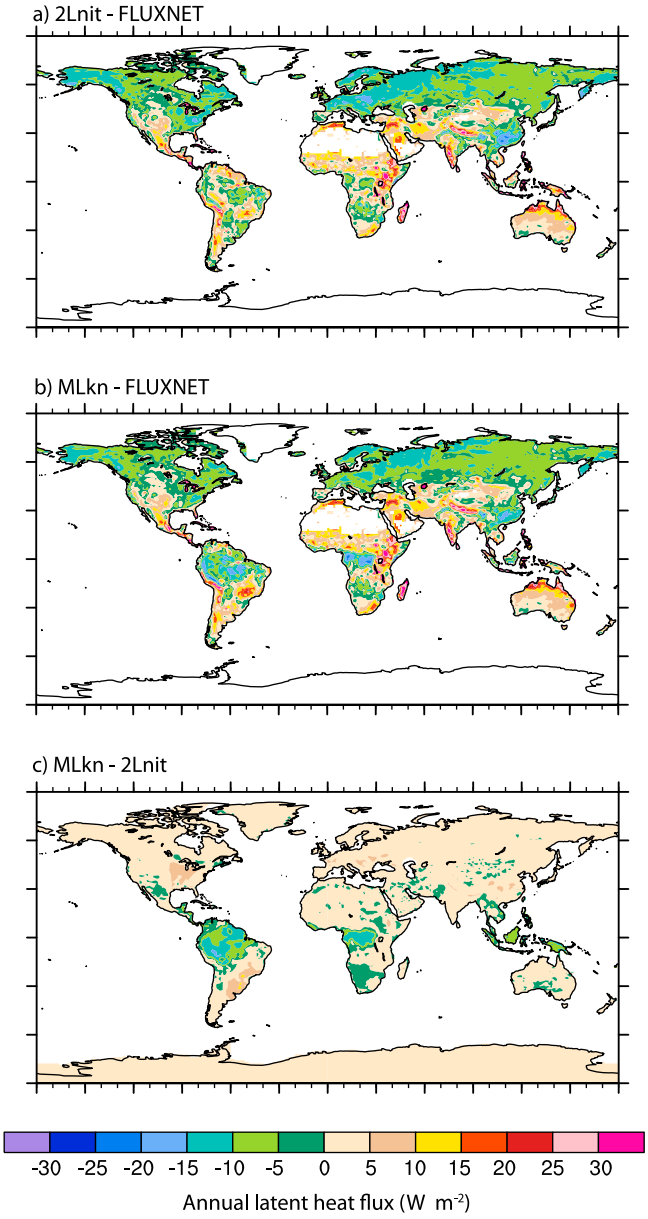

Figure 7. Annual latent heat flux (1982–2004) compared with FLUXNET estimates for simulations: (a) 2Lnit and (b) the multilayer canopy (MLkn). (c) Also shown is the difference MLkn - 2Lnit.

at all six sites, illustrated in Figure 8b for U.S.-WCr (see Figures S3 and S4 of the auxiliary material for all sites). The higher V_{cmax} in the 2Lobs simulation increases GPP and produces a better light-response curve at all sites, seen in decreased RMSE and increased GPP_{2000} relative to 2Lnit (Figure 10). The multilayer canopy (MLkn) lowers GPP and increases RMSE at 4 of 6 sites; RMSE is relatively unchanged at U.S.-UMB and U.S.-MMS. Overall, RMSE increases and GPP_{2000} bias increases in MLkn and MLjmx relative to 2Lobs (Figure 10).

[47] The 2Lnit simulation provides the best light-response curves for the four tropical evergreen broadleaf forest sites, illustrated in Figure 8c for BR-Ma2 (see Figure S5 of the auxiliary material for all sites), though GPP_{2000} is biased low (Figure 10). The lower observed V_{cmax} in the 2Lobs simulation degrades the light-response curves, seen in decreased GPP_{2000} and increased RMSE. The multilayer models (MLkn and MLjmx) further degrade the light-response curves with lower GPP_{2000} and higher RMSE.

[48] The 2Lnit simulation has low GPP at the four grassland sites, illustrated in Figure 9a for CA-Let (see Figure S6 of the auxiliary material for all sites). This matches FLUXNET for U.S.-FPe and U.S.-Bkg, but underestimates GPP for the more productive CA-Let and U.S.-ARc sites. High V_{cmax} in the 2Lobs simulation degrades the light-response curves, seen in increased RMSE and high GPP_{2000} (Figure 10), though U.S.-Arc is an exception. The multilayer models (MLkn and MLjmx) reduce GPP and improve the simulations with lower GPP_{2000} and reduced RMSE, except for U.S.-ARc.

[49] The 2Lnit simulation has low GPP at the four cropland sites, illustrated in Figure 9b for U.S.-Ne3 (see Figure S7 of the auxiliary material for all sites). High V_{cmax} in the 2Lobs simulation increases GPP and better matches the FLUXNET light-response curves, seen in reduced RMSE and higher GPP_{2000} (Figure 10). The multilayer models (MLkn and MLjmx) reduce GPP and therefore increase RMSE, but have comparatively little effect relative to 2Lobs and are still greatly improved compared with the 2Lnit simulation.

[50] All simulations overestimate canopy light use efficiency, except for evergreen broadleaf forest (α, Figure 10c). The greatest error occurs in boreal evergreen needleleaf forest with a bias of 0.05–0.06 μmol CO_2 J^{-1}. In other biomes, the bias is approximately 0.02–0.03 μmol CO_2 J^{-1}. The multilayer models (MLkn and MLjmx) decrease light use efficiency by about 0.01–0.02 μmol CO_2 J^{-1} compared with 2Lobs.

4. Discussion

[51] Values for the photosynthetic parameter V_{cmax} (at 25°C) in CLM4 are used to calculate a potential GPP that is additionally decreased for nitrogen availability. Annual GPP simulated without this nitrogen reduction (2Lpot) is much larger than FLUXNET estimates (Table 3, Figures 4a and 6a). Other studies have also found high GPP without the nitrogen reduction [*Thornton et al.*, 2007; *Bonan and Levis*, 2010; *Bonan et al.*, 2011]. Only when V_{cmax} is substantially reduced (2Lnit) is simulated annual GPP comparable to FLUXNET (Table 3, Figures 4a and 6b). Model simulation with the *Kattge et al.* [2009] observed V_{cmax} (2Lobs) similarly increases annual GPP compared with the lower V_{cmax} in the 2Lnit simulation and overestimates GPP compared with FLUXNET estimates, except in Amazonia (Table 3, Figures 4a and 6c).

[52] Analysis of light-response curves at 26 FLUXNET sites over a range of boreal, temperate, and tropical climates and forest, grassland, and cropland vegetation also highlight the discrepancy between the low nitrogen-reduced V_{cmax} and the observed V_{cmax}. At all locations, except the four tropical sites, observed V_{cmax} (2Lobs) gives higher photosynthetic capacity than in the nitrogen-reduced (2Lnit) simulation (GPP_{2000}, Figure 10).

[53] Simulations with the multilayer canopy provide insight to the cause of the high GPP bias. The GPP simulated

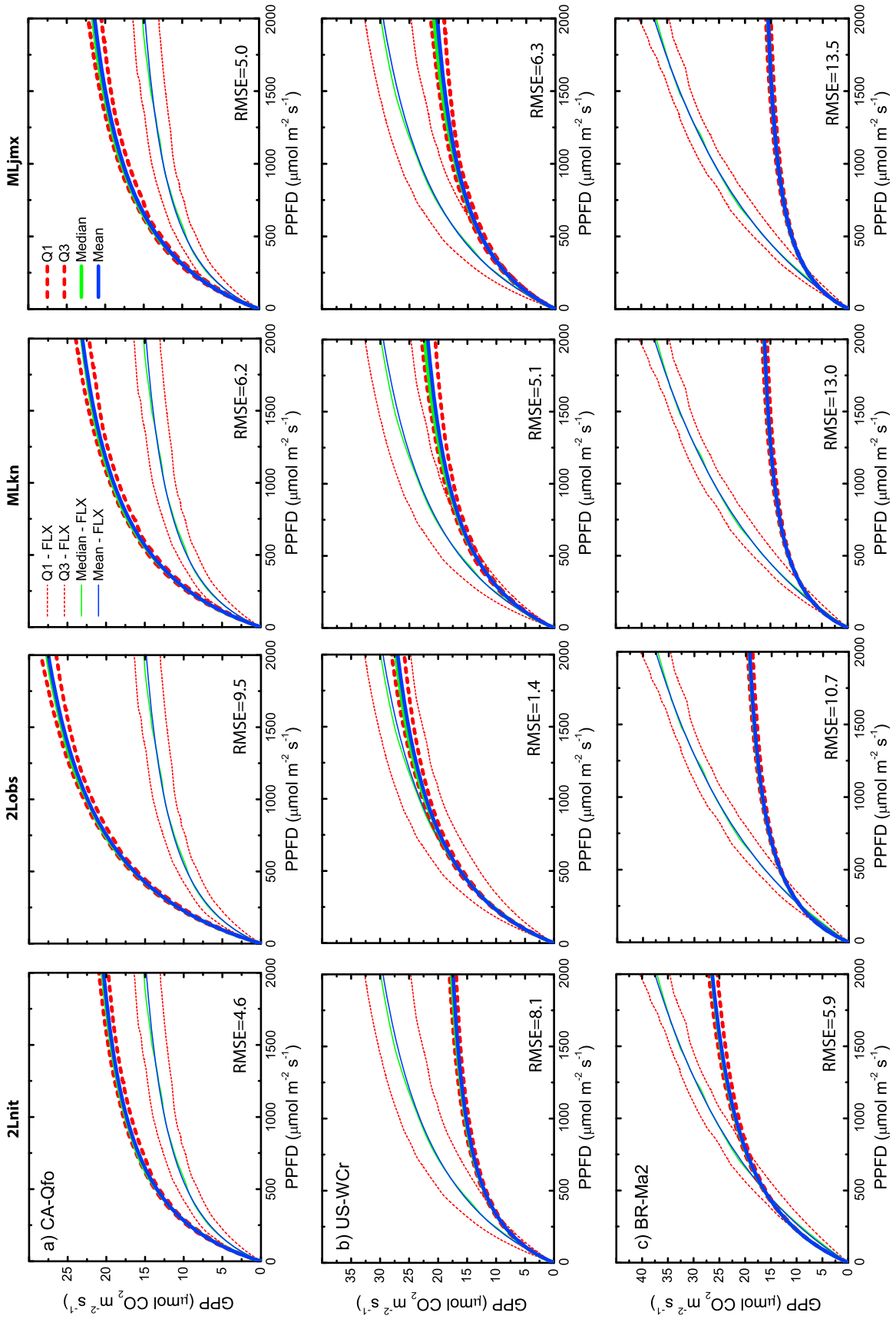
2Lnit
2Lobs
MLkn
MLjmx
a) CA-Qfo
b) US-WCr
c) BR-Ma2
RMSE=4.6
RMSE=9.5
RMSE=6.2
RMSE=5.0
RMSE=8.1
RMSE=1.4
RMSE=5.1
RMSE=6.3
RMSE=5.9
RMSE=10.7
RMSE=13.0
RMSE=13.5
Q1
Q3
Median
Mean
Q1 - FLX
Q3 - FLX
Median - FLX
Mean - FLX
GPP (μmol CO2 m-2 s-1)
PPFD (μmol m-2 s-1)

Figure 8

with the multilayer canopy matches that of the two-leaf canopy for low diffuse fraction or for high K_n, conditions under which shaded leaf photosynthesis is low (Figures 3a and 3g). However, with the low, but observationally constrained, values for K_n used in these simulations, the multilayer canopy has less GPP than the two-leaf canopy when the diffuse fraction is nonzero because the shaded leaves photosynthesize at a lower rate than in the two-leaf canopy (Figure 3d). As a result, the multilayer canopy reduces biases in annual GPP that are introduced with the use of observed $V_{c\max}$ (MLobs, Table 3, Figures 4b and 5). Further to this, adjusting K_n from a constant value of 0.11 to a value that varies with $V_{c\max}$ [*Lloyd et al.*, 2010] produces an additional small reduction in GPP (MLkn). Lower $J_{\max}$ relative to $V_{c\max}$, as in *Medlyn et al.* [2002], also reduces GPP (MLjmx). Biases in the MLkn simulation (and also MLjmx) compared with FLUXNET are comparable, though of opposite sign, to those in 2Lnit (Figures 6b and 6d).

[54] However, results of the light-response curves are mixed with regard to model performance (GPP_{2000} and RMSE, Figure 10). The most prominent improvement is boreal evergreen needleleaf forest, where observed $V_{c\max}$ (2Lobs) introduces large biases in the simulated light-response curves compared with the 2Lnit simulation, but the multilayer canopy (MLkn and MLjmx) reduces these biases, which also translates to reduced biases in annual GPP. Similar results are not seen in temperate evergreen needleleaf forest, but are seen in grassland.

[55] At other sites, improvement in the simulated light-response curves arises predominantly from observed $V_{c\max}$, not from the multilayer canopy (Figure 10). In deciduous broadleaf forest, for example, observed $V_{c\max}$ (2Lobs) substantially improves the light-response curves compared with 2Lnit. The multilayer canopy (MLkn and MLjmx) decreases GPP and substantially degrades the simulation at four of the six sites, though the simulations are still improved compared with 2Lnit.

[56] Cropland light-response curves are substantially improved with observed $V_{c\max}$, and the multilayer canopy has much smaller effect (Figure 10). The cropland simulations are dominated by the higher observed $V_{c\max}$ (101 μmol CO_2 m^{-2} s^{-1}) compared with the nitrogen-reduced $V_{c\max}$ (32 μmol CO_2 m^{-2} s^{-1}). *Levis et al.* [2012] also found that better fit to observed leaf area and turbulent fluxes required the higher *Kattge et al.* [2009] $V_{c\max}$ in CLM4 simulations with a prognostic crop growth model.

[57] Observed $V_{c\max}$ substantially degrades the simulation for Amazonian evergreen broadleaf forest, seen in both annual GPP (Figure 5a) and the light-response curves (Figures 8c and 10). The observed $V_{c\max}$ for tropical broadleaf evergreen trees (41 μmol CO_2 m^{-2} s^{-1}) is considerably lower than that used in the 2Lpot (72 μmol CO_2 m^{-2} s^{-1}) and 2Lnit (65 μmol CO_2 m^{-2} s^{-1}) simulations. Other modeling studies for Amazonia report a range of values for $V_{c\max}$, which tends toward higher than *Kattge et al.* [2009]: 43 μmol CO_2 m^{-2} s^{-1} [*Carswell et al.*, 2000]; 58 μmol CO_2 m^{-2} s^{-1} [*Mercado et al.*, 2006]; 64 μmol CO_2 m^{-2} s^{-1}, based on the *Lloyd et al.* [2010] analysis of *Domingues et al.* [2005]; and 68 μmol CO_2 m^{-2} s^{-1} [*Lloyd et al.*, 1995]. *Mercado et al.* [2009] used values of 32, 40, 47, 52, and 52 μmol CO_2 m^{-2} s^{-1} for five Amazonian sites, with good correspondence to observed light-response curves. *Fisher et al.* [2007], however, successfully used values of 24–44 μmol CO_2 m^{-2} s^{-1} for simulations in eastern Amazonia. The failure of the *Kattge et al.* [2009] $V_{c\max}$ and the multilayer canopy in our simulations warrants further study.

[58] Overall, the multilayer canopy (MLkn and MLjmx) is comparable to or better than the 2Lnit simulation when considering annual GPP (Table 4) and also light-response curves (Figure 10). The 2Lnit simulation has low error in annual GPP as well as some light-response curves (e.g., evergreen broadleaf forest), but $V_{c\max}$ is much different from the *Kattge et al.* [2009] estimates (Figure 1). Those observed $V_{c\max}$ values (2Lobs) improve some simulated light-response curves relative to 2Lnit (deciduous broadleaf forest and cropland), but degrade annual GPP. The multilayer canopy (MLkn), in conjuncture with the observed $V_{c\max}$, improves annual GPP compared with the 2Lobs simulation and is comparable to the 2Lnit simulations. The light-response curves are generally improved or comparable (less than 2 μmol CO_2 m^{-2} s^{-1} difference in RMSE) relative to the 2Lnit simulation (except evergreen broadleaf forest), and are improved (boreal evergreen needleleaf forest and grassland), comparable (cropland and temperate evergreen needleleaf forest), and degraded (deciduous broadleaf forest) relative to the 2Lobs simulation. Use of lower $J_{\max}$ (MLjmx) also decreases GPP and illustrates the sensitivity to $J_{\max}$.

[59] Better comparison with the upscaled annual GPP rather than the tower light-response curves may reflect site variability not captured in global terrestrial biosphere models. The FLUXNET upscaling filters some of the site specific characteristics of the flux towers such as soil nutrients, soil hydrology, phenotypic variability, and disturbance history [*Jung et al.*, 2010, 2011; *Beer et al.*, 2010]. Flux variability among sites due to these factors is smoothed in the upscaled product, but is present in the individual tower light-response curves.

[60] Much of the difference in simulated light-response curves from the FLUXNET data is related to photosynthetic capacity (GPP_{2000}, Figure 10b) rather than light use efficiency (α, Figure 10c). *Mercado et al.* [2009] found that light use efficiency is a key parameter when fitting their model to flux tower data, and model-data calibration might provide further insight to this parameter. Our simulations use a single value for $V_{c\max}$ (at 25°C) that varies among plant

Figure 8. Observed and simulated GPP light-response curves for representative sites: (a) CA-Qfo (evergreen needleleaf forest), (b) U.S.-WCr (deciduous broadleaf forest), and (c) BR-Ma2 (evergreen broadleaf forest). Shown are the FLUXNET (thin lines denoted FLX) and simulated (thick lines) statistical curves defined by the first and third quartiles (Q1 and Q3), median, and mean. Simulations are the two-leaf canopy with nitrogen-reduced $V_{c\max}$ (2Lnit) and with observed $V_{c\max}$ (2Lobs) and the multilayer canopy (MLkn and MLjmx). Shown is the root-mean-square error (RMSE) for each site, calculated using the observed and simulated mean light-response curve. Photosynthetic photon flux density (PPFD) is $0.5R_g \times 4.6$. Additional sites are shown in auxiliary material for evergreen needleleaf forest (Figures S1 and S2), deciduous broadleaf forest (Figures S3 and S4), and evergreen broadleaf forest (Figure S5).

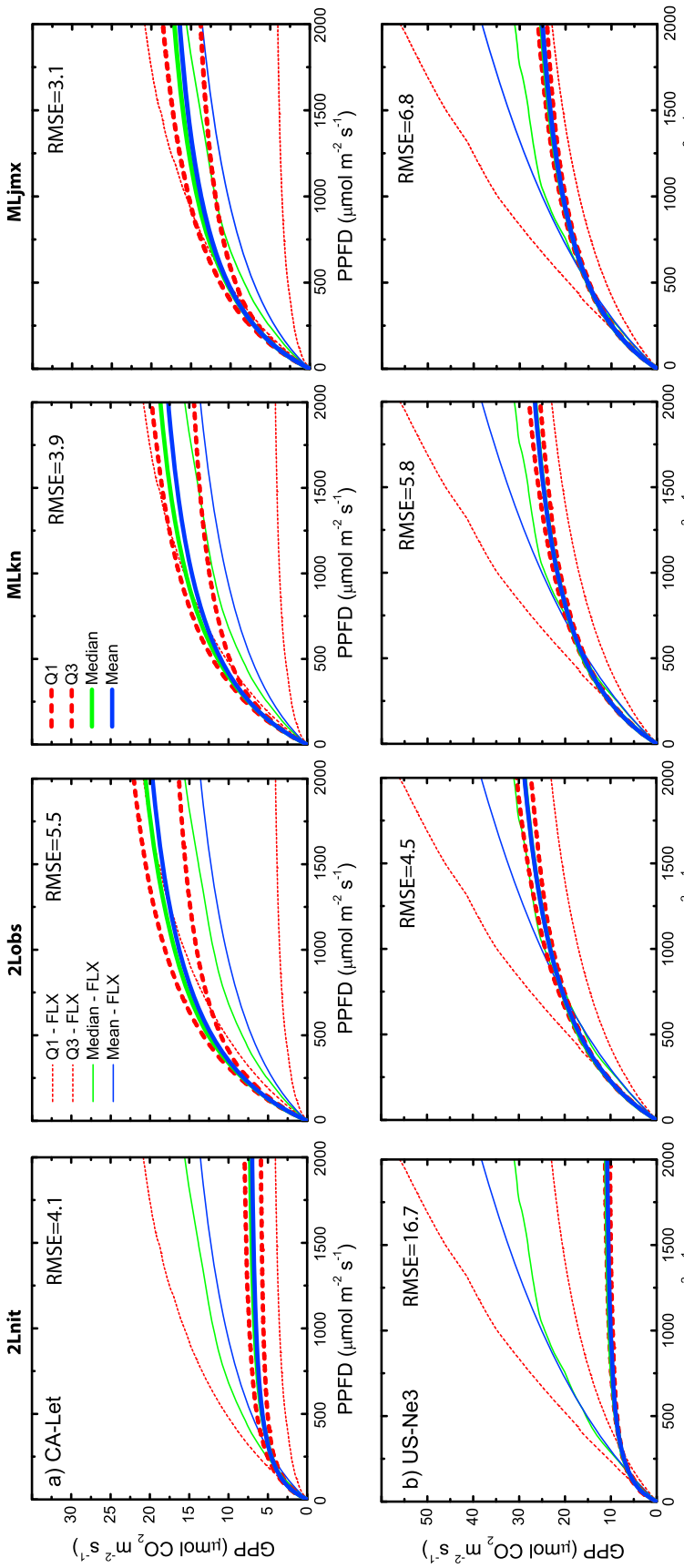

Figure 9. As in Figure 8, but for (a) CA-Let (grassland) and (b) U.S.-Ne3 (cropland). Additional sites are shown in auxiliary material for grassland (Figure S6) and cropland (Figure S7).

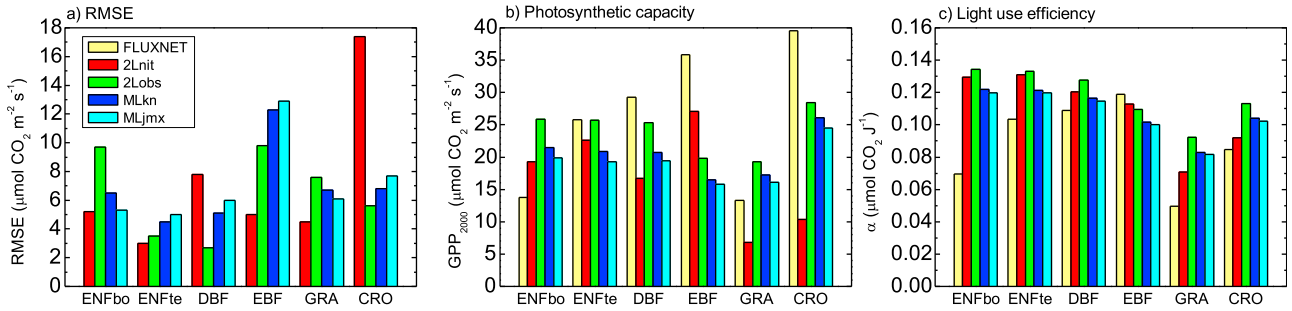

Figure 10. Light-response curve (a) root-mean-square error (RMSE), (b) photosynthetic capacity (GPP_{2000}), and (c) light use efficiency (α) for FLUXNET tower sites and model simulations. Values are calculated using the mean light-response curve at each site, and shown are the biome average values. Evergreen needleleaf forest is differentiated by boreal (bo) and temperate (te).

functional types, but not within a plant functional type. Yet the *Kattge et al.* [2009] estimates for $V_{c\max}$ have large variability within a plant functional type. Deviations from the FLUXNET tower light-response curves likely reflect, in part, lack of variability in $V_{c\max}$. Additionally, the FLUXNET light-response curves have much larger temporal variability than seen in the model simulations. Similar variability is observed in other analysis of light-response curves at an individual tower site [*Pilegaard et al.*, 2011].

[61] Our inability to fully match annual GPP estimates (Figures 4 and 5) and flux tower light-response curves (Figures 8 and 9) suggests that our ability to represent environmental and physiological controls of GPP in global terrestrial biosphere models is incomplete. While it is intellectually satisfying to scale from leaf to canopy, it is evident that such scaling is still not completely adequate in our model. Indeed, our simulations highlight a particular difficulty in representing light absorption by shaded leaves and within-canopy profiles of photosynthetic capacity (represented by the scaling parameter K_n). Model-data fusion techniques use eddy covariance flux data to calibrate models and constrain model parameters and provide a complementary approach to bottom-up, leaf to canopy scaling [*Wang et al.*, 2001, 2007; *Santaren et al.*, 2007; *Williams et al.*, 2009; *Ziehn et al.*, 2011]. However, if effective canopy parameters are estimated, the leaf-level information from trait databases such as *Kattge et al.* [2009, 2011] can hardly be used as prior information.

[62] In our simulations, explicitly resolved profiles of light and photosynthesis in the multilayer canopy produce results that differ from the two-leaf canopy. Previous studies using the Goudriaan radiation parameterization showed that a two-leaf canopy that differentiates between sunlit and shaded leaves, together with a vertical profile of $V_{c\max}$ represented through a gradient in foliage nitrogen specified by K_n, is a satisfactory simplification of a multilayer canopy [*de Pury and Farquhar*, 1997, 1999; *Wang and Leuning*, 1998, 1999]. Our analysis shows that this is true for sunlit leaves, but light absorption by shaded leaves, which receive only diffuse radiation, remains problematic if the canopy gradient in photosynthetic capacity is shallow (low K_n).

[63] The error between the two-leaf and multilayer canopy models increases with greater diffuse radiation [*de Pury and Farquhar*, 1997], seen also in our idealized canopy simulations (Figures 3a and 3d). This inaccuracy is reduced when photosynthetic capacity decreases sharply with canopy depth, such as with high values for K_n (Figure 3g). The studies of *de Pury and Farquhar* [1997] and *Wang and Leuning* [1998] both used higher values for K_n than in our simulations. In our idealized canopy simulations, the Goudriaan two-leaf and multilayer solutions are virtually indistinguishable with K_n = 0.5, as are the Norman solutions (Figure 3g). However, the K_n values in our global simulations are much smaller, either constant at K_n = 0.11 or varying from 0.13 to 0.23 depending on $V_{c\max}$, based on observational data [*Lloyd et al.*, 2010]. With larger K_n, the difference in annual GPP between the two-leaf and multilayer canopies decreases (Figure 4c).

[64] Our simulations have important implications for the CLM4 carbon-nitrogen biogeochemistry (CLM4CN). Much of the transient behavior of CLM4CN is caused by strong nitrogen down-regulation of GPP [*Thornton et al.*, 2007, 2009]. Our results suggest that the nitrogen limitation-induced reduction of GPP compensates for deficiency in the two-leaf canopy parameterization that produces high GPP. This deficiency is related to light absorption for shaded leaves and is accentuated with the low values for K_n used in the simulations. When the light profile and leaf traits are explicitly resolved in a multilayer canopy, GPP simulated using observed $V_{c\max}$ is comparable to the nitrogen down-regulated simulation, with the prominent exception of Amazonia (Figure 6).

[65] Additionally, the effect of nitrogen to decrease GPP in CLM4CN occurs independent of $V_{c\max}$ and the photosynthesis-stomatal conductance model, so that there is no direct effect of nitrogen availability on evapotranspiration and surface temperature. A more parsimonious parameterization of nitrogen-photosynthesis relationships would be to allow foliage nitrogen (and hence $V_{c\max}$) to vary in response to plant demand and plant uptake. In this framework, foliage nitrogen becomes an important validation of the simulated carbon-nitrogen biogeochemistry. Other models of the terrestrial biosphere for climate simulation use such an approach [*Wang et al.*, 2010; *Zaehle and Friend*, 2010].

[66] In addition to allowing a more correct simulation of photosynthesis when nitrogen scaling of photosynthetic capacity is shallow through the canopy (i.e., small K_n), the multilayer canopy additionally simulates vertical variation in

light and photosynthesis in the canopy, with strong implications for vegetation dynamics. A multilayer canopy resolves the depth at which light is insufficient to maintain a positive leaf carbon balance and therefore provides a physiological limit to leaf area. The CLM4CN carbon-nitrogen model does not have such a limit and can simulate leaf area index in excess of 20 m^2 m^{-2} [*Lawrence et al.*, 2011]. Furthermore, individual plant models of forest succession [*Botkin et al.*, 1972; *Shugart*, 1984; *Smith et al.*, 2001; *Sato et al.*, 2007] and cohort-based ecosystem demography models [*Moorcroft et al.*, 2001; *Medvigy et al.*, 2009; *Fisher et al.*, 2010] are built upon explicit competition for light. Adequate representation of light competition may well be required if terrestrial biosphere models are to fully capture vegetation dynamics.

[67] With recognition of the strong role terrestrial ecosystems have in regulating climate change, models of the global terrestrial biosphere are a central feature in the shift from climate models to earth system models. As such, the terrestrial biosphere modeling community has a responsibility to develop methodologies to comprehensively and quantitatively evaluate model performance. Several such frameworks have emerged in recent years to provide performance metrics [*Randerson et al.*, 2009; *Cadule et al.*, 2010; *Blyth et al.*, 2011]. These activities strive to define a standardized evaluation of models as a benchmark to assess model improvements. A common feature of these model benchmarks is comparison with monitoring data such as eddy covariance flux tower networks, ecological observation networks, global remote sensing, and atmospheric CO_2 measurement stations. Our analyses reported in *Bonan et al.* [2011] and continued here show that model evaluation of GPP must span multiple levels of system organization (e.g., leaf, canopy, and global) and must assess models for their consistency with process-level knowledge across scales.

5. Conclusions

[68] The CLM4 simulates GPP that is biased high compared with FLUXNET estimates. The revised model of *Bonan et al.* [2011] is greatly improved with respect to GPP (and also evapotranspiration), but the V_{cmax} values used in the model are less than those estimated by *Kattge et al.* [2009] for field vegetation, with the exception of tropical broadleaf evergreen trees. The simulations presented here show that this discrepancy in V_{cmax} arises from deficiencies in the CLM4 parameterization of the canopy as a sunlit and a shaded big-leaf. The deficiency is related to light absorption by shaded leaves that causes high photosynthetic rates, is accentuated when nitrogen scaling of photosynthetic capacity within the canopy is shallow (represented by the canopy scaling parameter K_n), and the inaccuracy is decreased with sharp decline in photosynthetic capacity (high K_n). The CLM4 has a shallow, but observationally constrained, within-canopy gradient in photosynthetic capacity. The imposed nitrogen down-regulation of GPP compensates for this deficiency in the two-leaf canopy parameterization that produces high GPP.

[69] Model structural deficiencies can be compensated by parameter adjustment, which may explain the lack of consensus in values for V_{cmax} used in global models of the terrestrial biosphere. Model benchmarking activities must evaluate terrestrial biosphere models not only in their fidelity to monitoring data sets of the biosphere, but also in terms of model parameters and model structure. In this context, global databases of leaf traits (V_{cmax}), within-canopy profiles of photosynthetic capacity (K_n), eddy covariance flux measurements at individual FLUXNET towers, and global flux fields empirically upscaled from FLUXNET towers provide important complementary information to constrain global terrestrial biosphere models.

[70] **Acknowledgments.** The National Center for Atmospheric Research is sponsored by the National Science Foundation. This work was supported by National Science Foundation grants AGS-1020767 and EF-1048481.

References

Baldocchi, D. D., and K. B. Wilson (2001), Modeling CO_2 and water vapor exchange of a temperate broadleaved forest across hourly to decadal time scales, *Ecol. Modell.*, *142*, 155–184, doi:10.1016/S0304-3800(01)00287-3.

Baldocchi, D. D., K. B. Wilson, and L. Gu (2002), How the environment, canopy structure and canopy physiological functioning influence carbon, water and energy fluxes of a temperate broad-leaved deciduous forest-an assessment with the biophysical model CANOAK, *Tree Physiol.*, *22*, 1065–1077, doi:10.1093/treephys/22.15-16.1065.

Ball, J. T., I. E. Woodrow, and J. A. Berry (1987), A model predicting stomatal conductance and its contribution to the control of photosynthesis under different environmental conditions, in *Progress in Photosynthesis Research*, vol. 4, edited by J. Biggins, pp. 221–224, Martinus Nijhoff, Dordrecht, Netherlands.

Beer, C., et al. (2010), Terrestrial gross carbon dioxide uptake: Global distribution and covariation with climate, *Science*, *329*, 834–838, doi:10.1126/science.1184984.

Beerling, D. J., and W. P. Quick (1995), A new technique for estimating rates of carboxylation and electron transport in leaves of C_3 plants for use in dynamic global vegetation models, *Global Change Biol.*, *1*, 289–294, doi:10.1111/j.1365-2486.1995.tb00027.x.

Bernacchi, C. J., E. L. Singsaas, C. Pimentel, A. R. Portis Jr., and S. P. Long (2001), Improved temperature response functions for models of Rubisco–limited photosynthesis, *Plant Cell Environ.*, *24*, 253–259, doi:10.1111/j.1365-3040.2001.00668.x.

Best, M. J., et al. (2011), The Joint UK Land Environment Simulator (JULES), model description: Part 1: Energy and water fluxes, *Geosci. Model Dev.*, *4*, 677–699, doi:10.5194/gmd-4-677-2011.

Blyth, E., D. B. Clark, R. Ellis, C. Huntingford, S. Los, M. Pryor, M. Best, and S. Sitch (2011), A comprehensive set of benchmark tests for a land surface model of simultaneous fluxes of water and carbon at both the global and seasonal scale, *Geosci. Model Dev.*, *4*, 255–269, doi:10.5194/gmd-4-255-2011.

Bonan, G. B. (2008), Forests and climate change: Forcings, feedbacks, and the climate benefits of forests, *Science*, *320*, 1444–1449, doi:10.1126/science.1155121.

Bonan, G. B., and S. Levis (2010), Quantifying carbon-nitrogen feedbacks in the Community Land Model (CLM4), *Geophys. Res. Lett.*, *37*, L07401, doi:10.1029/2010GL042430.

Bonan, G. B., P. J. Lawrence, K. W. Oleson, S. Levis, M. Jung, M. Reichstein, D. M. Lawrence, and S. C. Swenson (2011), Improving canopy processes in the Community Land Model version 4(CLM4) using global flux fields empirically inferred from FLUXNET data, *J. Geophys. Res.*, *116*, G02014, doi:10.1029/2010JG001593.

Botkin, D. B., J. F. Janak, and J. R. Wallis (1972), Some ecological consequences of a computer model of forest growth, *J. Ecol.*, *60*, 849–872, doi:10.2307/2258570.

Cadule, P., P. Friedlingstein, L. Bopp, S. Sitch, C. D. Jones, P. Ciais, S. L. Piao, and P. Peylin (2010), Benchmarking coupled climate-carbon models against long-term atmospheric CO_2 measurements, *Global Biogeochem. Cycles*, *24*, GB2016, doi:10.1029/2009GB003556.

Carswell, F. E., P. Meir, E. V. Wandelli, L. C. M. Bonates, B. Kruijt, E. M. Barbosa, A. D. Nobre, J. Grace, and P. G. Jarvis (2000), Photosynthetic capacity in a central Amazonian rain forest, *Tree Physiol.*, *20*, 179–186, doi:10.1093/treephys/20.3.179.

Collatz, G. J., J. T. Ball, C. Grivet, and J. A. Berry (1991), Physiological and environmental regulation of stomatal conductance, photosynthesis and transpiration: A model that includes a laminar boundary layer, *Agric. For. Meteorol.*, *54*, 107–136, doi:10.1016/0168-1923(91)90002-8.

Collatz, G. J., M. Ribas-Carbo, and J. A. Berry (1992), Coupled photosynthesis-stomatal conductance model for leaves of C_4 plants, *Aust. J. Plant Physiol.*, *19*, 519–538, doi:10.1071/PP9920519.

Dai, Y., R. E. Dickinson, and Y.-P. Wang (2004), A two–big–leaf model for canopy temperature, photosynthesis, and stomatal conductance, *J. Clim.*, *17*, 2281–2299, doi:10.1175/1520-0442(2004)017<2281:ATMFCT>2.0.CO;2.

de Pury, D. G. G., and G. D. Farquhar (1997), Simple scaling of photosynthesis from leaves to canopies without the errors of big-leaf models, *Plant Cell Environ.*, *20*, 537–557, doi:10.1111/j.1365-3040.1997.00094.x.

de Pury, D. G. G., and G. D. Farquhar (1999), A commentary on the use of a sun/shade model to scale from the leaf to a canopy, *Agric. For. Meteorol.*, *95*, 257–260.

Domingues, T. F., J. A. Berry, L. A. Martinelli, J. P. H. B. Ometto, and J. R. Ehleringer (2005), Parameterization of canopy structure and leaf-level gas exchange for an eastern Amazonian tropical rain forest (Tapajós National Forest, Pará, Brazil), *Earth Interact.*, *9*(17), 1–23, doi:10.1175/EI149.1.

Ethier, G. J., and N. J. Livingston (2004), On the need to incorporate sensitivity to CO_2 transfer conductance into the Farquhar-von Caemmerer-Berry leaf photosynthesis model, *Plant Cell Environ.*, *27*, 137–153, doi:10.1111/j.1365-3040.2004.01140.x.

Farquhar, G. D., S. von Caemmerer, and J. A. Berry (1980), A biochemical model of photosynthetic CO_2 assimilation in leaves of C_3 species, *Planta*, *149*, 78–90, doi:10.1007/BF00386231.

Fisher, R. A., M. Williams, A. Lola da Costa, Y. Malhi, R. F. da Costa, S. Almeida, and P. Meir (2007), The response of an eastern Amazonian rain forest to drought stress: Results and modelling analyses from a throughfall exclusion experiment, *Global Change Biol.*, *13*, 2361–2378, doi:10.1111/j.1365-2486.2007.01417.x.

Fisher, R., N. McDowell, D. Purves, P. Moorcroft, S. Sitch, P. Cox, C. Huntingford, P. Meir, and F. I. Woodward (2010), Assessing uncertainties in a second-generation dynamic vegetation model caused by ecological scale limitations, *New Phytol.*, *187*, 666–681, doi:10.1111/j.1469-8137.2010.03340.x.

Goudriaan, J. (1977), *Crop Micrometeorology: A Simulation Study*, 249 pp., Cent. for Agric. Publ. and Doc., Wageningen, Netherlands.

Goudriaan, J., and H. H. van Laar (1994), *Modelling Potential Crop Growth Processes: Textbook with Exercises*, 238 pp., Kluwer Acad., Dordrecht, Netherlands.

Jung, M., et al. (2010), Recent decline in the global land evapotranspiration trend due to limited moisture supply, *Nature*, *467*, 951–954, doi:10.1038/nature09396.

Jung, M., et al. (2011), Global patterns of land-atmosphere fluxes of carbon dioxide, latent heat, and sensible heat derived from eddy covariance, satellite, and meteorological observations, *J. Geophys. Res.*, *116*, G00J07, doi:10.1029/2010JG001566.

Kattge, J., and W. Knorr (2007), Temperature acclimation in a biochemical model of photosynthesis: A reanalysis of data from 36 species, *Plant Cell Environ.*, *30*, 1176–1190, doi:10.1111/j.1365-3040.2007.01690.x.

Kattge, J., W. Knorr, T. Raddatz, and C. Wirth (2009), Quantifying photosynthetic capacity and its relationship to leaf nitrogen content for global-scale terrestrial biosphere models, *Global Change Biol.*, *15*, 976–991, doi:10.1111/j.1365-2486.2008.01744.x.

Kattge, J., et al. (2011), TRY: A global database of plant traits, *Global Change Biol.*, *17*, 2905–2935, doi:10.1111/j.1365-2486.2011.02451.x.

Lasslop, G., M. Reichstein, D. Papale, A. D. Richardson, A. Arneth, A. Barr, P. Stoy, and G. Wohlfahrt (2010), Separation of net ecosystem exchange into assimilation and respiration using a light response curve approach: Critical issues and global evaluation, *Global Change Biol.*, *16*, 187–208, doi:10.1111/j.1365-2486.2009.02041.x.

Lawrence, D. M., et al. (2011), Parameterization improvements and functional and structural advances in version 4 of the Community Land Model, *J. Adv. Model. Earth Syst.*, *3*, M03001, doi:10.1029/2011MS000045.

Leuning, R. (2002), Temperature dependence of two parameters in a photosynthesis model, *Plant Cell Environ.*, *25*, 1205–1210, doi:10.1046/j.1365-3040.2002.00898.x.

Leuning, R., F. M. Kelliher, D. G. G. de Pury, and E.-D. Schulze (1995), Leaf nitrogen, photosynthesis, conductance and transpiration: Scaling from leaves to canopy, *Plant Cell Environ.*, *18*, 1183–1200, doi:10.1111/j.1365-3040.1995.tb00628.x.

Levis, S., G. B. Bonan, E. Kluzek, P. E. Thornton, A. Jones, W. J. Sacks, and C. J. Kucharik (2012), Interactive crop management in the Community Earth System Model (CESM1), Seasonal influences on land-atmosphere fluxes, *J. Clim.*, doi:10.1175/JCLI-D-11-00446.1, in press.

Lloyd, J., and J. A. Taylor (1994), On the temperature dependence of soil respiration, *Funct. Ecol.*, *8*, 315–323, doi:10.2307/2389824.

Lloyd, J., J. Grace, A. C. Miranda, P. Meir, S. C. Wong, H. S. Miranda, I. R. Wright, J. H. C. Gash, and J. McIntyre (1995), A simple calibrated model of Amazon rainforest productivity based of leaf biochemical properties, *Plant Cell Environ.*, *18*, 1129–1145, doi:10.1111/j.1365-3040.1995.tb00624.x.

Lloyd, J., et al. (2010), Optimisation of photosynthetic carbon gain and within-canopy gradients of associated foliar traits for Amazon forest trees, *Biogeosciences*, *7*, 1833–1859, doi:10.5194/bg-7-1833-2010.

Medlyn, B. E., et al. (2002), Temperature response of parameters of a biochemically based model of photosynthesis. II. A review of experimental data, *Plant Cell Environ.*, *25*, 1167–1179, doi:10.1046/j.1365-3040.2002.00891.x.

Medvigy, D., S. C. Wofsy, J. W. Munger, D. Y. Hollinger, and P. R. Moorcroft (2009), Mechanistic scaling of ecosystem function and dynamics in space and time: Ecosystem demography model version 2, *J. Geophys. Res.*, *114*, G01002, doi:10.1029/2008JG000812.

Mercado, L., J. Lloyd, F. Carswell, Y. Malhi, P. Meir, and A. D. Nobre (2006), Modelling Amazonian forest eddy covariance data: A comparison of big leaf versus sun/shade models for the C-14 tower at Manus. I. Canopy photosynthesis, *Acta Amazon.*, *36*, 69–82, doi:10.1590/S0044-59672006000100009.

Mercado, L. M., C. Huntingford, J. H. C. Gash, P. M. Cox, and V. Jogireddy (2007), Improving the representation of radiation interception and photosynthesis for climate model applications, *Tellus, Ser. B*, *59*, 553–565.

Mercado, L. M., J. Lloyd, A. J. Dolman, S. Sitch, and S. Patiño (2009), Modelling basin-wide variations in Amazon forest productivity: Part 1: Model calibration, evaluation and upscaling functions for canopy photosynthesis, *Biogeosciences*, *6*, 1247–1272, doi:10.5194/bg-6-1247-2009.

Moorcroft, P. R., G. C. Hurtt, and S. W. Pacala (2001), A method for scaling vegetation dynamics: The ecosystem demography model (ED), *Ecol. Monogr.*, *71*, 557–586, doi:10.1890/0012-9615(2001)071[0557:AMFSVD]2.0.CO;2.

Norman, J. M. (1979), Modeling the complete crop canopy, in *Modification of the Aerial Environment of Plants*, edited by B. J. Barfield and J. F. Gerber, pp. 249–277, Am. Soc. Agric. Eng., St. Joseph, Mich.

Oleson, K. W., et al. (2010), Technical description of version 4.0 of the Community Land Model (CLM), *Tech. Note NCAR/TN-478+STR*, 257 pp., Natl. Cent. for Atmos. Res., Boulder, Colo.

Pilegaard, K., A. Ibrom, M. S. Courtney, P. Hummelshoj, and N. O. Jensen (2011), Increasing net CO_2 uptake by a Danish beech forest during the period from 1996 to 2009, *Agric. For. Meteorol.*, *151*, 934–946, doi:10.1016/j.agrformet.2011.02.013.

Randerson, J. T., et al. (2009), Systematic assessment of terrestrial biogeochemistry in coupled climate-carbon models, *Global Change Biol.*, *15*, 2462–2484, doi:10.1111/j.1365-2486.2009.01912.x.

Santaren, D., P. Peylin, N. Viovy, and P. Ciais (2007), Optimizing a process-based ecosystem model with eddy-covariance flux measurements: A pine forest in southern France, *Global Biogeochem. Cycles*, *21*, GB2013, doi:10.1029/2006GB002834.

Sato, H., A. Itoh, and T. Kohyama (2007), SEIB-DGVM: A new dynamic global vegetation model using a spatially explicit individual-based approach, *Ecol. Modell.*, *200*, 279–307, doi:10.1016/j.ecolmodel.2006.09.006.

Shugart, H. H. (1984), *A Theory of Forest Dynamics: The Ecological Implications of Forest Succession Models*, 278 pp., Springer, New York.

Smith, B., I. C. Prentice, and M. T. Sykes (2001), Representation of vegetation dynamics in the modelling of terrestrial ecosystems: Comparing two contrasting approaches within European climate space, *Global Ecol. Biogeogr.*, *10*, 621–637, doi:10.1046/j.1466-822X.2001.00256.x.

Thornton, P. E., and N. E. Zimmermann (2007), An improved canopy integration scheme for a land surface model with prognostic canopy structure, *J. Clim.*, *20*, 3902–3923, doi:10.1175/JCLI4222.1.

Thornton, P. E., J.-F. Lamarque, N. A. Rosenbloom, and N. M. Mahowald (2007), Influence of carbon-nitrogen cycle coupling on land model response to CO_2 fertilization and climate variability, *Global Biogeochem. Cycles*, *21*, GB4018, doi:10.1029/2006GB002868.

Thornton, P. E., et al. (2009), Carbon-nitrogen interactions regulate climate-carbon cycle feedbacks: Results from an atmosphere-ocean general circulation model, *Biogeosciences*, *6*, 2099–2120, doi:10.5194/bg-6-2099-2009.

Wang, Y.-P. (2000), A refinement to the two-leaf model for calculating canopy photosynthesis, *Agric. For. Meteorol.*, *101*, 143–150, doi:10.1016/S0168-1923(99)00165-3.

Wang, Y.-P., and R. Leuning (1998), A two-leaf model for canopy conductance, photosynthesis and partitioning of available energy. I: Model description and comparison with a multi-layered model, *Agric. For. Meteorol.*, *91*, 89–111, doi:10.1016/S0168-1923(98)00061-6.

Wang, Y.-P., and R. Leuning (1999), Reply to a commentary on the use of a sun/shade model to scale from the leaf to canopy by D.G.G. de Pury and G.D. Farquhar, *Agric. For. Meteorol.*, *95*, 261–265.

Wang, Y. P., R. Leuning, H. A. Cleugh, and P. A. Coppin (2001), Parameter estimation in surface exchange models using nonlinear inversion: How many parameters can we estimate and which measurements are

most useful?, *Global Change Biol.*, *7*, 495–510, doi:10.1046/j.1365-2486.2001.00434.x.

Wang, Y. P., D. Baldocchi, R. Leuning, E. Falge, and T. Vesala (2007), Estimating parameters in a land-surface model by applying nonlinear inversion to eddy covariance flux measurements from eight FLUXNET sites, *Global Change Biol.*, *13*, 652–670, doi:10.1111/j.1365-2486.2006.01225.x.

Wang, Y. P., R. M. Law, and B. Pak (2010), A global model of carbon, nitrogen and phosphorus cycles for the terrestrial biosphere, *Biogeosciences*, *7*, 2261–2282, doi:10.5194/bg-7-2261-2010.

Wang, Y. P., E. Kowalczyk, R. Leuning, G. Abramowitz, M. R. Raupach, B. Pak, E. van Gorsel, and A. Luhar (2011), Diagnosing errors in a land surface model (CABLE) in the time and frequency domains, *J. Geophys. Res.*, *116*, G01034, doi:10.1029/2010JG001385.

Williams, M., et al. (2009), Improving land surface models with FLUXNET data, *Biogeosciences*, *6*, 1341–1359, doi:10.5194/bg-6-1341-2009.

Wohlfahrt, G. (2004), Modelling fluxes and concentrations of CO_2, H_2O and sensible heat within and above a mountain meadow canopy: A comparison of three Lagrangian models and three parameterisation options for the Lagrangian time scale, *Boundary Layer Meteorol.*, *113*, 43–80, doi:10.1023/B:BOUN.0000037326.40490.1f.

Wohlfahrt, G., M. Bahn, U. Tappeiner, and A. Cernusca (2001), A multicomponent, multi-species model of vegetation-atmosphere CO_2 and energy exchange for mountain grasslands, *Agric. For. Meteorol.*, *106*, 261–287, doi:10.1016/S0168-1923(00)00224-0.

Wullschleger, S. D. (1993), Biochemical limitations to carbon assimilation in C_3 plants: A retrospective analysis of the A/C_i curves from 109 species, *J. Exp. Bot.*, *44*, 907–920, doi:10.1093/jxb/44.5.907.

Zaehle, S., and A. D. Friend (2010), Carbon and nitrogen cycle dynamics in the O-CN land surface model: 1. Model description, site-scale evaluation, and sensitivity to parameter estimates, *Global Biogeochem. Cycles*, *24*, GB1005, doi:10.1029/2009GB003521.

Ziehn, T., J. Kattge, W. Knorr, and M. Scholze (2011), Improving the predictability of global CO_2 assimilation rates under climate change, *Geophys. Res. Lett.*, *38*, L10404, doi:10.1029/2011GL047182.